



PERGAMON

Deep-Sea Research II 50 (2003) 57–86

---

---

DEEP-SEA RESEARCH  
PART II

---

---

www.elsevier.com/locate/dsr2

## The Cape Cauldron: a regime of turbulent inter-ocean exchange

Olaf Boebel<sup>a,b,c,\*</sup>, Johann Lutjeharms<sup>c</sup>, Claudia Schmid<sup>d</sup>, Walter Zenk<sup>e</sup>,  
Tom Rossby<sup>b</sup>, Charlie Barron<sup>f</sup>

<sup>a</sup> Alfred Wegener Institute for Polar and Marine Research, PO 120161, Bremerhaven 27515, Germany

<sup>b</sup> Graduate School of Oceanography, University of Rhode Island, 02882 Narragansett, RI, USA

<sup>c</sup> Department of Oceanography, University of Cape Town, 7701 Rondebosch, South Africa

<sup>d</sup> Cooperative Institute for Marine and Atmospheric Studies, University of Miami, 4301 Rickenbacker Causeway, FL 33149, USA

<sup>e</sup> Institut für Meereskunde an der Christian-Albrechts-Universität Kiel, Düsternbrooker Weg 20, 24105 Kiel, Germany

<sup>f</sup> Naval Research Laboratory, Stennis Space Center, 39529 MS, USA

Received 18 April 2002; accepted 26 July 2002

---

### Abstract

Combining in-situ Lagrangian intermediate depth velocity measurements from the KAPEX (Cape of Good Hope Experiments) float program with sea-surface height data, this study reviews the inter-ocean exchange mechanisms around southern Africa. In the southeastern Cape Basin, a highly energetic field of coexisting anticyclonic and cyclonic eddies is documented. Agulhas Rings of typically 200 km diameter are observed to merge, split, deform, and to reconnect to the Agulhas Retroflection. Concomitant, slightly smaller cyclones are observed to drift across the northwestward migration path of the Agulhas Rings. These cyclones, with typical diameters of 120 km, are formed within the Cape Basin along the African shelf, inshore of the Agulhas Current, and in the subantarctic region south of Africa.

The data suggest the annual formation of 3–6 long-lived Agulhas Rings that eventually cross 5°E longitude, while approximately twice the number of rings occur in the southeastern Cape Basin. Within this region, cyclones outnumber anticyclones by a factor of 3:2. Both cyclones and anticyclones extend through the upper thermocline into the intermediate depth layer. Mean drifts of anticyclones are  $3.8 \pm 1.2 \text{ cm s}^{-1}$  to the northwest, while cyclones follow a west–southwestward route at  $3.6 \pm 0.8 \text{ cm s}^{-1}$ . Transport estimates suggest that the intermediate depth layer in the southeastern Cape Basin is primarily supplied from the east (approximately 9 Sv), with minor direct inflow from the Atlantic to the west and south.

Cyclone/anticyclone interaction is surmised to result in vigorous stirring and mixing processes in the southeastern Cape Basin, which necessitates a review of the traditional concept of Indo-Atlantic inter-ocean exchange. We propose to limit the concept of “isolated Agulhas Rings embedded in a sluggish Benguela Drift” to the northwestern Cape Basin and beyond, while linking this regime to the Agulhas Retroflection proper through a zone of turbulent stirring and mixing in the southeastern Cape Basin, named for the first time the “Cape Cauldron” hereinafter.

© 2002 Elsevier Science Ltd. All rights reserved.

---

\*Corresponding author. Alfred Wegener Institute for Polar and Marine Research, PO 120161, Bremerhaven 27515, Germany. Tel.: +49-471-4831-1879; fax: +49-471-4831-1797.

E-mail addresses: oboebel@awi-bremerhaven.de (O. Boebel).

## 1. Introduction

Past descriptions of the inter-ocean exchange between the Indian and Atlantic Oceans at the Agulhas Retroflexion (Fig. 1) suggested this transport to be dominated by the migration of Agulhas Rings from the Agulhas Retroflexion through the Cape Basin into the western South Atlantic (see Lutjeharms, 1996 for a summary of observational studies). The shedding of Agulhas Rings was generally thought to follow a rather straightforward kinematic process. Representative for many other studies, Gründlingh (1995, p. 24,977) stated: “The spawning of a ring is preceded by a westward protrusion of the Agulhas Current and terminated when subantarctic water wedges northward to occlude the ring”. In his study, the Agulhas Retroflexion (the westernmost protrusion of the Agulhas Current where it folds back to the east) is suggested to slowly progress westward on the time scale of a few months. When reaching a critical extension, the protrusion was believed to become unstable and to shed an Agulhas Ring, which would move off into the Cape Basin. During this event the Agulhas Retroflexion would fall

back onto its easternmost position, only to start the process over again. However the dynamics governing the shedding were obscure and only recently did modeling efforts (see de Ruijter et al., 1999 for a review of modeling studies) achieve realistic results, such as the numbers of rings per year, or the observed nonperiodic Agulhas Ring shedding pattern (Treguier et al., 2003).

The Agulhas Rings emerging out of this spawning process were believed to then move with the steadily flowing Benguela Drift into the interior Cape Basin and to veer successively westwards, following a quasi-zonal path across the South Atlantic. While the Benguela Drift would be dominated by water from the South Atlantic (Garzoli and Gordon, 1996), “*isolated rings of Agulhas water west of the retroflexion*” (Gordon, 1986, p. 5043) would carry the bulk of Indian Ocean influence, which slowly would leak from the rings into the surrounding waters. Alternative inter-ocean exchange mechanisms, such as a possible direct inflow via narrow coast and shelf edge jet-like currents (Stramma and Peterson, 1989) (also called filaments), were deemed intermittent (Duncombe Rae et al., 1996)

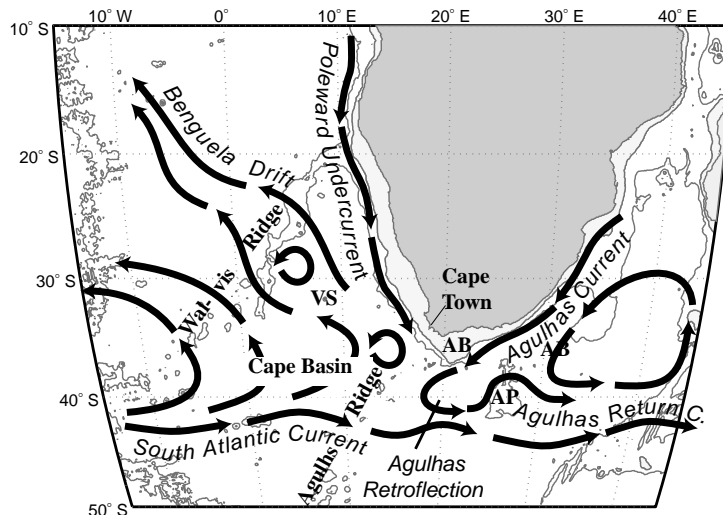


Fig. 1. Schematic of the traditional view of oceanic flow patterns around southern Africa for the upper and intermediate water layers. Oceanic features are labeled in italics, geographic features in regular font. The Cape Basin is circumscribed by the Walvis Ridge, the African East coast, the Agulhas Ridge and the southern extreme of the Mid-Atlantic Ridge. Two Agulhas Rings are depicted in the Cape Basin at 29°S and 38°S. The Agulhas Bank is the shaded shelf region to the south of Cape Town (AB), the Agulhas Plateau (AP) the shallow topographic feature near 40°S, 26°E. Vema Seamount (VS) is indicated. Topography is delineated by the 0, 1000 and 3000 m isobaths.

and to provide not more than 15% of the overall mass flux (Lutjeharms and Cooper, 1996).

Based on this concept, researchers estimated the inter-ocean exchange by calculating the heat and salt anomaly contained within a ring relative to a suitably chosen reference station nearby, but outside of the ring. The anomalies were then multiplied with the number of rings shed per year to estimate the annual mean transport (Byrne et al., 1994; Duncombe Rae et al., 1996; Goñi et al., 1997). Duncombe Rae et al. (1996), for example, estimated a minimum of 4–6 eddies of Agulhas origin to enter the Cape Basin per year during the 1992–1993 Benguela Sources and Transports (BEST) program. The mean available heat (AHA) and salt (ASA) anomaly per eddy was estimated to  $0.55 \times 10^{20}$  J and  $3.5 \times 10^{12}$  kg per year, with the total eddy field responsible for 2.6–3.8 Sv ( $1 \text{ Sverdrup, Sv} = 1 \times 10^6 \text{ m}^3 \text{ s}^{-1}$ ).<sup>1</sup>

The basis of these calculations was the concept that the “...Benguela Current transport consisted of a nearly steady flow confined between the South African coast and approximately 4°E ... and a more transient flow ... between 4°E and Walvis Ridge” (Garzoli et al., 1999, p. 20,971). In the vertical, these studies described the Benguela Current to involve the thermocline and Antarctic Intermediate Water (AAIW) layers, while a southward flow was suggested below (Garzoli and Gordon, 1996). The observed variability in the eastern part was predominantly assigned to the presence of energetic anticyclonic eddies, i.e. Agulhas Rings, however, cyclonic eddies had already been observed as well.

Stramma and Peterson (1990), based on the 1983 R.V. *Knorr* hydrographic section, showed a cyclone near 39°S, 11°E. The BEST hydrographic program identified 2 cyclones in 1992 and another 2 in 1993. Spanning the period between the BEST hydrographic surveys, inverted echosounder (IES) records (Watts and Rossby, 1977) furthermore showed “a seemingly persistent phenomenon is

what appears to be a ‘recoil’ effect in the [IES] record; that is, the thermocline appears to shallow appreciably after passage of an [anticyclonic] eddy before relaxing to the local mean” (Duncombe Rae et al., 1996, p. 11,958). In the same publication however, Duncombe Rae et al. (1996) chose to downplay the cyclones’ role in the area (p. 11,955): “We anticipate, however, that they [cyclones] will form only a small proportion of the eddy spectrum since mechanisms for their generation in the region are limited and the Cape Basin eddy field is dominated by the energetic Agulhas eddies”.

The skepticism of these authors towards their own observations of cyclones is probably due to two reasons. First, cyclonic eddies were strongly undersampled during BEST, prohibiting the determination of their amplitude or origin (Duncombe Rae et al., 1996), and hence reducing the amount of discussion dedicated to these features. Second, at the time of these experiments, anticyclonic Agulhas Rings were *the* topic of the day in this region. Due to their size and intensity they had been the eminent feature distinguishable (for short periods only) by sea-surface temperature measurements (Lutjeharms, 1981) and presented then one of the most accessible targets for the nascent satellite-borne altimetric measurements (Byrne et al., 1994; Gründlingh, 1995). At the same time, Agulhas Rings were of direct relevance to the emerging climate change discussion (Gordon, 1986; Lutjeharms and Gordon, 1987; Clement and Gordon, 1995). Consequently most hydrographic surveys of the time concentrated on these anticyclonic features<sup>2</sup> to provide ground truth for the exciting remotely sensed data.

However, it is not only the influx from the Indian Ocean that influences the Cape Basin dynamics. Previous Lagrangian studies in the western South Atlantic (Boebel et al., 1999)

<sup>1</sup>Note the difference in “eddy” transport, i.e. anomaly per feature times translation speed of feature, as used in this and other observational studies, while modeling studies define eddy transport as that part of the transport not contained in the mean transport. The paper by Treguier et al. (2003) discusses this difference in more detail.

<sup>2</sup>A similar focus on anticyclonic eddies occurred in many contemporaneous studies of the Mediterranean Outflow in the northeastern North Atlantic. A recent review of eddy abundance in the Canary and Iberian Basins by Richardson et al. (2000) however corrects this view by noting that about 1/3 of the eddies observed in the AMUSE program, which was the only experiment to feature an unbiased float seeding scheme, were cyclonic.

showed two quasi-zonal branches of the subtropical gyre dominating the circulation at intermediate depth near the Mid-Atlantic Ridge. The South Atlantic Current brings fresh AAIW from the Brazil–Malvinas Confluence Zone into the southern Cape Basin, while to the north, at about 30°S, a westward flow band appears to drain the latter (Schmid et al., 2000). While the two limbs are joined in the west by the Brazil Current to form one half of the subtropical gyre, its closure in the East remained obscure. Several possibilities, or any combination thereof, exist for the location of this missing link: A closure to the west of the Mid-Atlantic Ridge (Siedler et al., 1996), a closure within the Cape Basin (Stramma and England, 1999), or a closure via a detour through the Southwest Indian Ocean subgyre (Gordon et al., 1992).

With the AAIW minimum salinity changing only little over the entire width of the South Atlantic along the gyre's southern and northern zonal branches, which are separated by only about 1000 km, the observed salinity difference between these of about 0.1 (PSU) is quite remarkable. At 5°W, You et al.'s (2003) map of Antarctic Intermediate Water core salinity (their Fig. 3c), shows a salinity of 34.25 at 40°S and 34.35 at 30°S. No 'tongue', suggestive of an advective pathway connecting the two regimes, is visible. Analogous observations can be made in oxygen saturation on the shallow  $\sigma_0 = 26.61$  surface (Garzoli et al., 1999) (their plate 8), with values of 0.9 along 40°S and 0.8 along 30°S. Hence, if a direct link should exist between the northern and southern branch of the subtropical gyre, one is left wondering what processes are involved and how the water is modified so significantly over a relatively short distance.

In order to address in a systematic way the exchange of waters between the SE Atlantic and SW Indian Ocean, three float projects joined forces in an endeavor known as the Cape of Good Hope Experiments, KAPEX (Boebel et al., 1998). This paper focuses on the kinematics of the circulation in the southeastern Cape Basin through a combination of Lagrangian RAFOS float trajectories and altimetric sea-surface height data. An important finding of this study will be the role played by the cyclones, their interaction with the Agulhas

Rings, and their impact on the inter-ocean exchange.

Our paper proceeds by describing the float (RAFOS) and altimetric (MODAS-2D SSH) data, and their processing to extract trajectories of cyclonic and anticyclonic eddies. Then fields of kinetic energy are calculated to define the "Cape Cauldron" region. After discussing the properties of cyclonic and anticyclonic eddies the paper uses the float trajectories, in combination with altimetry, to arrive at a modified concept of the flow patterns around Southern Africa. The Appendix discusses the implications of this modified view on the calculation of inter-oceanic transport from Agulhas Ring property anomalies.

## 2. Data and data processing

### 2.1. RAFOS data

High-resolution trajectories, obtained at either 12- or 24-h intervals, of neutrally buoyant RAFOS floats (Rossby et al., 1986) drifting between 200 and 1350 m depth, were measured in the oceans surrounding southern Africa. Each position fix was accompanied by a concurrent measurement of ambient pressure and temperature. A detailed description of float deployments, data acquisition, and tracking procedures are given in Boebel et al. (2000).

From subsurface float position vectors of latitude and longitude, piecewise polynomial forms of cubic smoothing splines were calculated independently (using MATLAB™ Spline Toolbox function "csaps" with the smoothing parameter set to 0.5). The smoothing reduces positional jitter (due to tidal and inertial oscillations) on shorter than daily time scales, while mesoscale signals, which are the focus of this paper, are maintained. The smoothing has proven to be particularly useful, if not necessary, when calculating the second order derivatives to estimate curvature vorticity, as discussed below. A final visual comparison of each smoothed trajectory with its original showed that the mesoscale signals were not infringed upon by the procedure.

First- and second-order derivatives of the trajectories were directly obtained by forming the *analytical* derivatives of the set of polynomials describing each spline function, (using MATLAB™ Spline Toolbox function “fnder”.) The resulting six piecewise polynomial splines (for latitude ( $y$ ), longitude ( $x$ ) and their respective first and second derivatives) were then evaluated at 24-h intervals (regardless of the floats original data-sampling period). From these, float velocities and curvature vorticity were estimated. In comparison with the alternative use of “centered differences” to estimate velocity, the above approach offers advantages in that the resulting velocity is less prone to underestimation and that the lengths of velocity-, curvature vorticity-, and float position vectors remain constant, matching those of concurrent measurements of pressure and temperature. The trajectory curvature  $\kappa_t$  was estimated according to (Bower and Rossby, 1989) (dots indicate partial temporal derivatives):

$$\kappa_t = \frac{(\dot{x}\ddot{y} - \ddot{x}\dot{y})}{(\dot{x}^2 + \dot{y}^2)^{3/2}}$$

From this, an estimate of streamline curvature  $\kappa_s$  can be made (Bower, 1989):

$$\kappa_s = \kappa_t \frac{|\vec{v}|}{(|\vec{v}| - c)}$$

with  $|\vec{v}|$  being the float speed. Similar to Bower (1989) we chose a constant value for the phase velocity  $c$ , though our choice was  $c = 0 \text{ cm s}^{-1}$ , i.e. zero phase velocity throughout. In some cases, where a float stayed for several revolutions in a coherent eddy, it would have been possible to estimate the individual phase velocity  $c$  of this feature. However, for most of the float data the assignment of a phase velocity would remain highly ambiguous, because the float either is located between features or displays only a partial revolution. To avoid inconsistencies in the data processing,  $\kappa_s$  is hence approximated by  $\kappa_t$ , which should be sufficiently accurate within the statistical view taken below. From streamline curvature, curvature vorticity is then estimated as  $|\vec{v}| \cdot \kappa_s$ .

For further analysis, only data with associated pressure records between 650 and 1150 dbar, i.e. the horizon of Atlantic and Indian Ocean inter-

mediate waters (Shannon and Hunter, 1988), were accepted. Fig. 2 shows the resulting RAFOS float trajectories, color-coded according to their associated curvature vorticity. To further extract the pathways of coherent eddies from the tangle of float trajectories, additional screening had to be applied:

- (1) Each float position was flagged “anticyclonic” or “cyclonic” according to its associated curvature vorticity  $|\vec{v}| \cdot \kappa_s$  while simultaneously meeting the condition  $||\vec{v}| \cdot \kappa_s| > 0.05 \times 10^{-5} \text{ s}^{-1}$  (Fig. 2, red segments = anticyclonic; blue segments = cyclonic).
- (2) Each streak of trajectory data that remained “anticyclonic” or “cyclonic” for at least 40 days, with possible intermediate gaps of negligible ( $||\vec{v}| \cdot \kappa_s| \leq 0.05 \times 10^{-5} \text{ s}^{-1}$ ) or reverse curvature vorticity not exceeding 10 days, was assumed to represent a coherent eddy.
- (3) Finally, the average curvature vorticity over all data points within the resulting segment had to exceed  $0.05 \times 10^{-5} \text{ s}^{-1}$  for the respective segment to be retained for further analysis.

Trajectory segments selected in such manner are depicted in Fig. 3. The top two panels depict anticyclonic trajectory segments (left) and the resulting overall float displacement (right), while the bottom panels present the same information for cyclones.

## 2.2. MODAS-2D SSH data

Sea-surface height data from the TOPEX/Poseidon and ERS satellites were processed at the Stennis Space Center’s Naval Research Laboratory. Being a component of the center’s Modular Ocean Data Assimilation System (MODAS), MODAS-2D generates daily, mesoscale-resolving, absolute sea-surface steric height anomalies from a combination of ocean climatology and objectively mapped quasi-instantaneous altimetric measurements (Jacobs et al., 2001; Fox et al., 2003), which are referenced to as MODAS-2D SSH or simply SSH herein. In the accompanying paper by Boebel and Barron (2003), it is shown statistically that the SSH appropriately represents

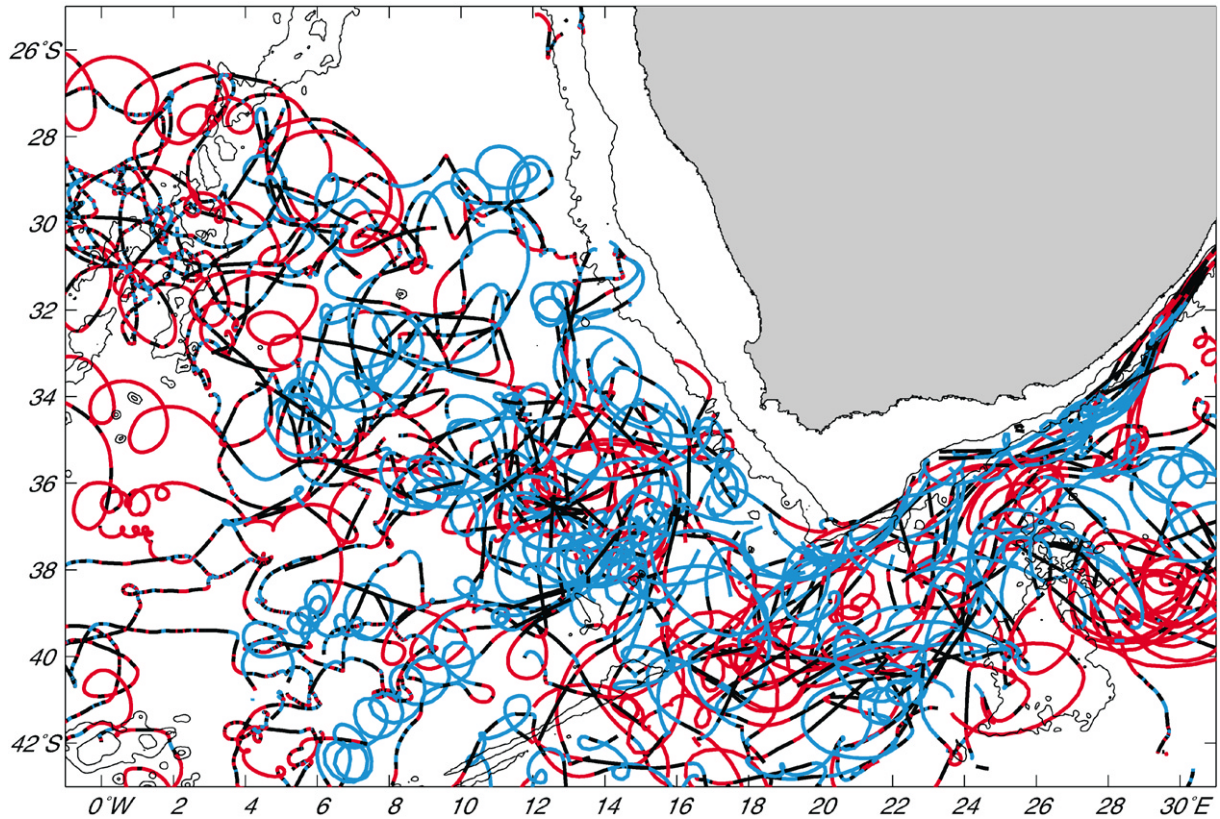


Fig. 2. Anticyclonic (red, 13,335 float days), cyclonic (blue, 11,873 float days) and below threshold ( $\kappa_t < 0.05 \times 10^{-5} \text{ s}^{-1}$ ; black, 7882 float days) RAFOS float trajectory segments. The 0, 1000 and 3000 m isobaths are shown by thin black lines.

the mesoscale cyclonic and anticyclonic features in the southeastern corner of the Cape Basin as well as, to the verifiable degree, instantaneous geostrophic surface velocities. The direct visual comparison of SSH and float trajectories, as presented in the accompanying movie,<sup>3</sup> further shows a close resemblance of the surface (MODAS-derived) and

intermediate (RAFOS-derived) mesoscale kinematic patterns.

Fig. 4 shows the mean (top) and standard deviation ( $\sigma$ , bottom) of SSH, averaged over the 1997–1999 3-year KAPEX period. SSH in the top figure clearly outlines the Agulhas Retroflexion, with an average eastward extension to 21°E, i.e. due south of Cape Agulhas. The 1.5 m contour, shown in white on both plots, has proved to be a good proxy for the location of the Agulhas Return Current as it emerges out of the Retroflexion (Boebel et al., 2003). The bottom panel of SSH variability shows the anticipated high variability ( $> 0.3 \text{ m}$ ) in the Agulhas Retroflexion. This variability, to a large extent, is due to the zonal displacement of the Agulhas Retroflexion proper and has been reported on numerous occasions. A tongue of increased variability ( $\sigma > 0.2 \text{ m}$ ) extends into the Cape Basin from the gap between the

<sup>3</sup>Four movies associated with this publication can be obtained by request from the corresponding author or downloaded from Elsevier's DSR-II web portal at <http://www.elsevier.com/locate/dsr2>. Please follow the links to this issue's table of content where electronic annexes are linked. The movies are provided as zip archive (cape\_cauldron.avi.zip) of 48 Mbyte size. The movies contained are:

- the\_cape\_cauldron\_ssh.avi;
- the\_cape\_cauldron\_agulhas\_cyclone.avi;
- the\_cape\_cauldron\_subantarctic\_cyclone.avi;
- the\_cape\_cauldron\_upwelling\_cyclone.avi.

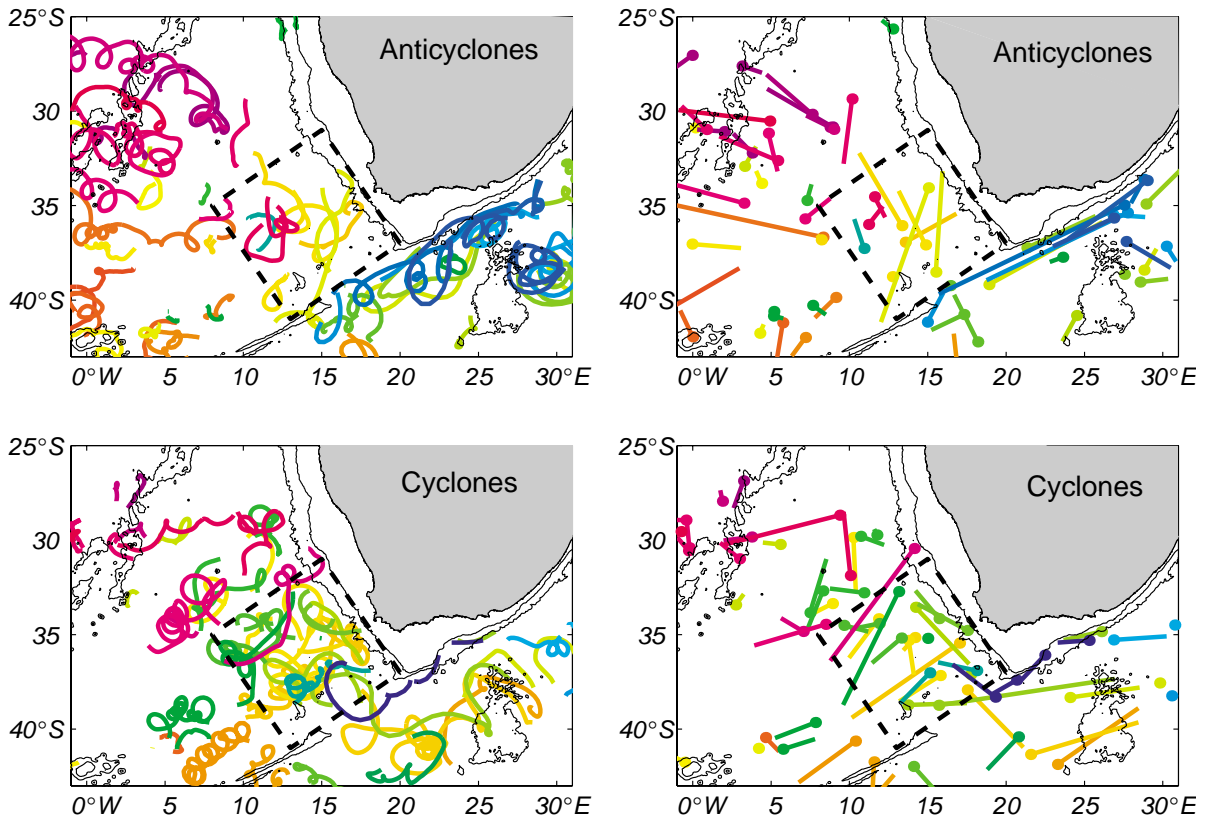


Fig. 3. Selected RAFOS float trajectories and displacement vectors of floats caught in coherent eddy structures. Displacement vectors begin at the dot. See text for detailed selection criteria. Isobaths are at 0, 1000 and 3000 m. The dashed box defined the Cape Cauldron region as selected for the statistics given in the text.

southernmost tip of the Agulhas Bank and the Schmitt-Ott Seamount (i.e. the northwestern corner of the Agulhas Ridge). It is limited to 35°S in its northward extension.

To follow coherent mesoscale features in the MODAS-2D SSH during the 1997–1999 period, daily positions of relative SSH extremes were calculated. The locations of maximums were established by contouring the sea-surface height repeatedly at decreasing levels. The process started at an elevation of 2.15 m, a value above all observed values. While repeating the processes at  $-5$  cm steps, eventually the first closed contours (circles), representative of eddy peaks, emerged. The center of each closed contour was recorded. When, while contouring at successively lower levels, more closed contour lines (circles) emerged,

a check was performed whether the new circle would engulf a previously found maximum. If so, no record was made, but if not, another peak position was added to the list. This process was repeated down to the 1.55 m elevation.

This process allows finding local peaks of varying height, and even distinguishes between multiple peaks within larger eddies. This method appears superior to a simple search for SSH data points exceeding a threshold elevation since it compensates for some of the fluctuations introduced through the MODAS-2D interpolation schemes, and of possible additional SSH fluctuations due to the steric expansion of the water column (only an average seasonal signal was subtracted from the SSH data). For cyclones, the same approach was applied bottom up, i.e. from

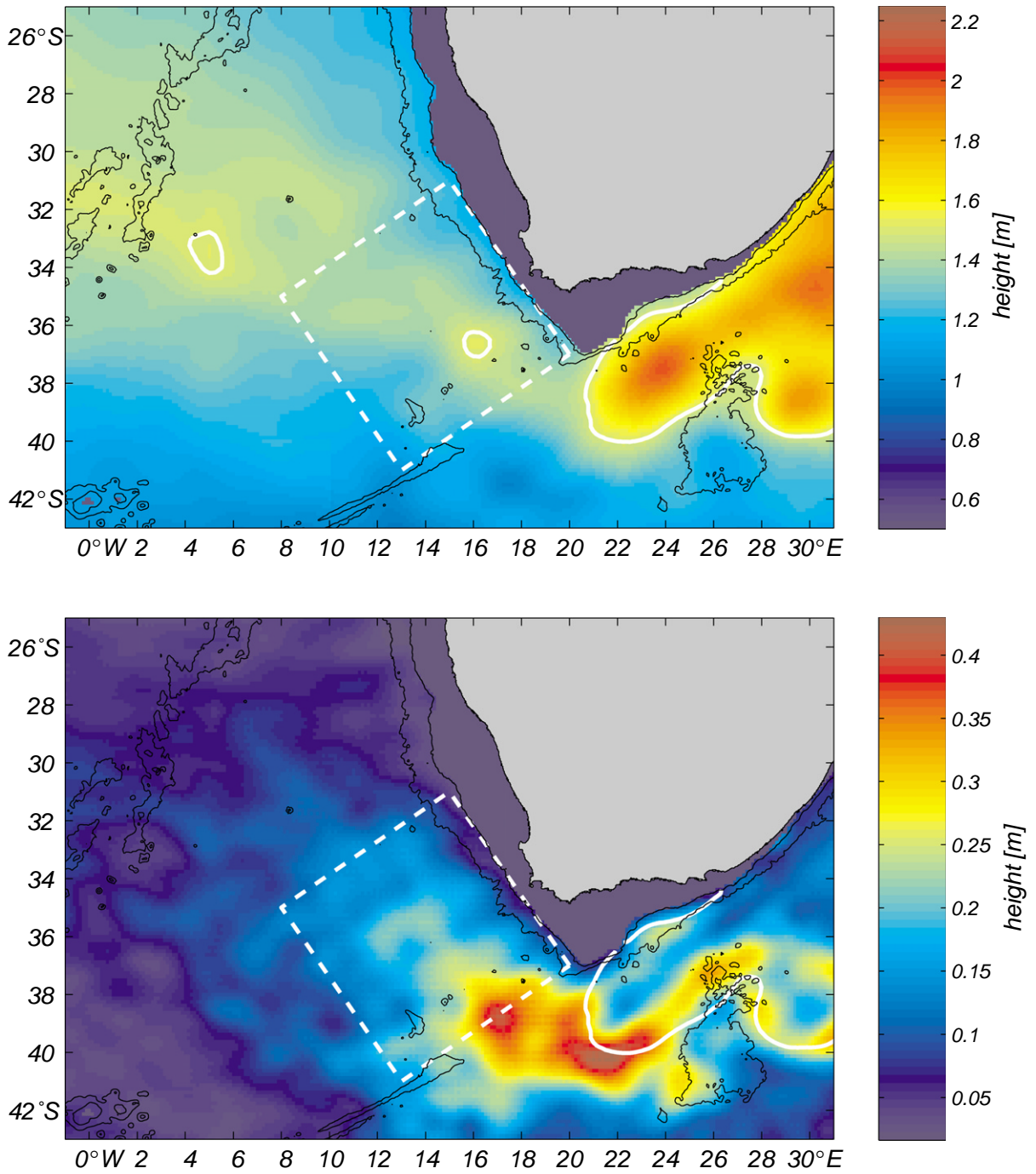


Fig. 4. Three-year mean (top) and standard deviation (bottom) from MODAS-2D SSH data. White contours in both plots give the position of the 1.5 m mean SSH. The dashed white box outlines the Cape Caution.

0.80 m at +5 cm intervals to 1.20 m. These first steps resulted in two arrays of cyclone and anticyclone positions versus time. However, so far the resulting positions were not linked in time, i.e. assigned to specific eddies, and a criterion had to be developed to connect positions from one day to the next.

For this, it is reasonable to exploit the fact that coherent vortices move continuously through space-time, or in other words, successive eddy positions should be in close proximity. Our analysis allows for a maximum distance between successive data points of 100 km, which is approximately the radius of an Agulhas Ring. Positions exceeding this distance were considered to belong to separate features. We also demanded that the eddy is traceable for at least 60 consecutive days in a row, excluding some intermittent splitting events. At last, to allow for an intermediate loss of tracking of the eddy, possibly caused by its unfortunate location between satellite ground tracks, we allowed for a maximum gap of 30 days between successive positions while maintaining the spatial restriction for the two positions to lie within 100 km. Figs. 5 and 6 show the resulting trajectories of anticyclones and cyclones in the Cape Cauldron after applying a smoothing spline function to the trajectory. Before continuing with a detailed discussion of these trajectories, however, it seems appropriate to characterize the region of interest in a kinematic sense. The results will then be used to define the geographical limits of subsequent statistical bulk estimates of eddy properties.

### 3. Defining the Cape Cauldron

Mean and eddy kinetic surface energy levels were calculated for the Cape Basin using daily surface velocity estimates derived from the SSH fields, assuming a purely geostrophic balance (Fu and Chelton, 2001). Based on these estimates, Fig. 7 shows the Eulerian mean kinetic energy density (MKE, top) and eddy kinetic energy density (EKE, bottom), calculated for each

MODAS-2D data point according to:

$$\text{MKE} = \frac{1}{2}\rho(\bar{u}^2 + \bar{v}^2) \text{ and } \text{EKE} = \frac{1}{2}\rho(u'^2 + v'^2)$$

with

$$v = \bar{v} + v', u = \bar{u} + u',$$

where  $u$  and  $v$  are the zonal and meridional components of the velocity, and  $\rho$  is the density. The bars indicate strictly temporal means and the primes indicate the deviation from those means. The averaging is performed over time from 1 January 1997–31 December 1999 for each  $1/8^\circ \times 1/8^\circ$  grid point individually and not over a space-time domain, as below for the corresponding calculation for RAFOS floats.<sup>4</sup> Fig. 7 (top panel) clearly depicts the Agulhas Current (AC), the Retroreflection proper and the Agulhas Return Current as features of increased mean kinetic energy ( $\text{MKE} > 50 \text{ J m}^{-3}$ ). Little of this mean energy leaks into the South Atlantic, or specifically the Cape Basin. In contrast, significant EKE is present in the southeastern part of the Cape Basin ( $\approx 50 \text{ J m}^{-3}$ , Table 1) and along the cyclonic side (to the right of the downstream coordinate) of the increased MKE levels of the Agulhas Current system.

A homologous analysis has been performed on  $2^\circ \times 2^\circ$  box averaged RAFOS float velocities (Fig. 8). The float data (selected as described above) were binned and the mean velocity calculated individually for each box and velocity component:

$$\bar{u}_b = \sum_{i \text{ in box } b} u_i \quad \bar{v}_b = \sum_{i \text{ in box } b} v_i$$

with  $i$  running over all float-days within a given box ( $b$ ), which results in a mixed space-time average. Perturbation velocities were derived for each box “ $b$ ” by

$$u'_b = \sum_{i \text{ in box } b} (u_i - \bar{u}_b) \quad v'_b = \sum_{i \text{ in box } b} (v_i - \bar{v}_b).$$

The resulting Lagrangian intermediate depth MKE distribution shows MKE levels of the order of  $1 \text{ J m}^{-3}$  in the Cape Basin, similar to the lower

<sup>4</sup>The water density  $\rho$  was approximated by  $1000 \text{ kg m}^{-3}$ . To convert the resulting unit of ( $\text{J m}^{-3}$ ) to the alternatively used unit ( $\text{cm}^2 \text{ s}^{-2}$ ), multiply the value listed herein by 10.

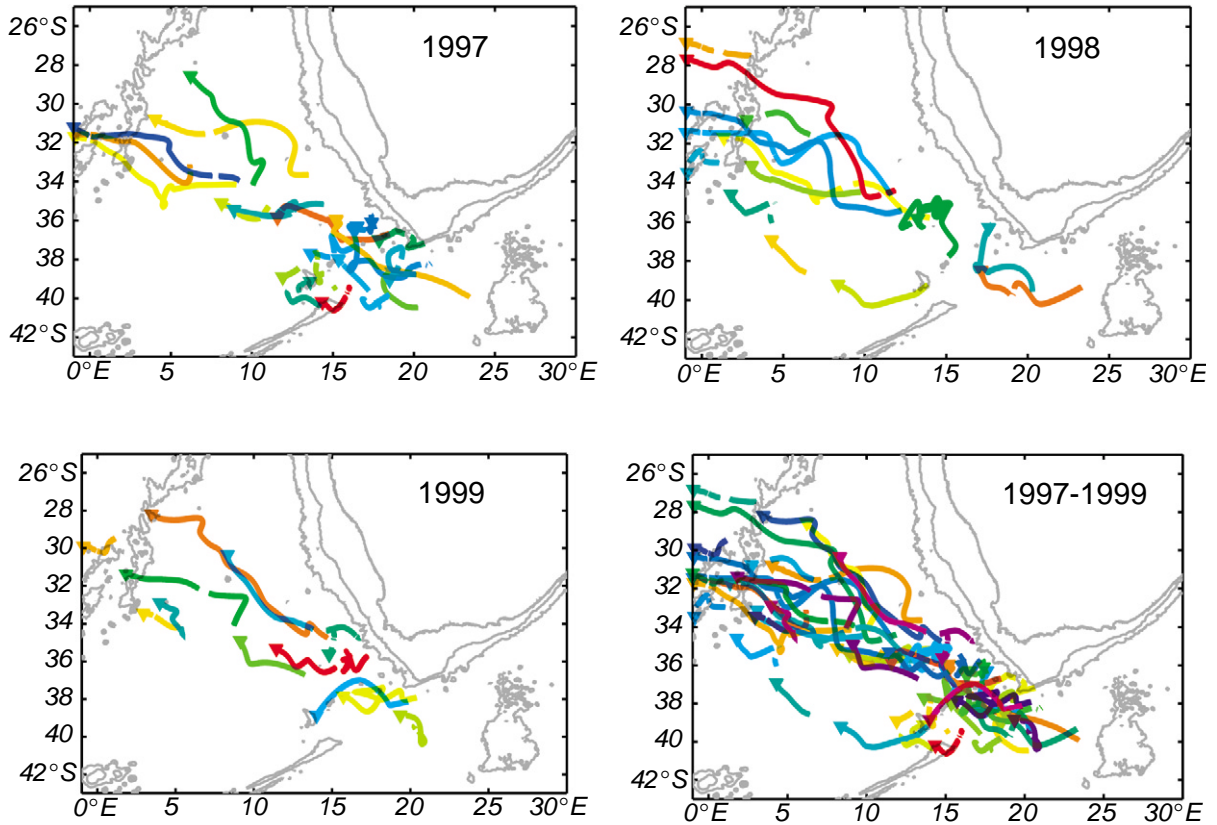


Fig. 5. Trajectories of anticyclones in the Cape Cauldron as estimated from MODAS-2D SSH for the years 1997–1999 individually and accumulatively. Eddies that exist solely to the east of 20°E or south of 40°S are excluded. Eddy trajectories end at the triangle. Isobaths as in Fig. 1.

end of surface EKE observed for this region. The float EKE near the gap between the Agulhas Bank and the northeastern corner of the Agulhas Ridge reaches levels comparable to the mean surface EKE of the order of  $100 \text{ J m}^{-3}$ , with levels higher than  $10 \text{ J m}^{-3}$  found throughout the remainder of the tongue of increased variability.

The high EKE region directly contiguous to the Agulhas Current system, between 37° and 41°S and east of 19°E, is dominated by variability introduced by the zonal protrusion and contraction of the retroflection as already mentioned in the description of SSH variability (Fig. 4). In contrast, the southeastern part of the Cape Basin is characterized, at both surface and intermediate depth levels by a high eddy to mean kinetic energy ratio paired with a mean flow undistinguishable

from zero. We here suggest, for the first time, labeling this region “Cape Cauldron”, with “Cape” referring to its geographical location in the Cape Basin and near Cape of Good Hope, while “Cauldron” suggests an oceanographic regime of turbulent mixing and stirring. It should be noted that the “Cape Cauldron”, being located northwest of the Agulhas Retroflection proper, is geographically separate from what is commonly understood as the Agulhas Retroflection region.

While an exact definition of the “Cape Cauldron” region, based on an objective criteria such as the ratio between MKE and EKE, is conceivable, such detail is of little practical use. It appears sufficient for our purpose to realize the existence of such a regime and to delineate roughly its location. For further analysis, based on a

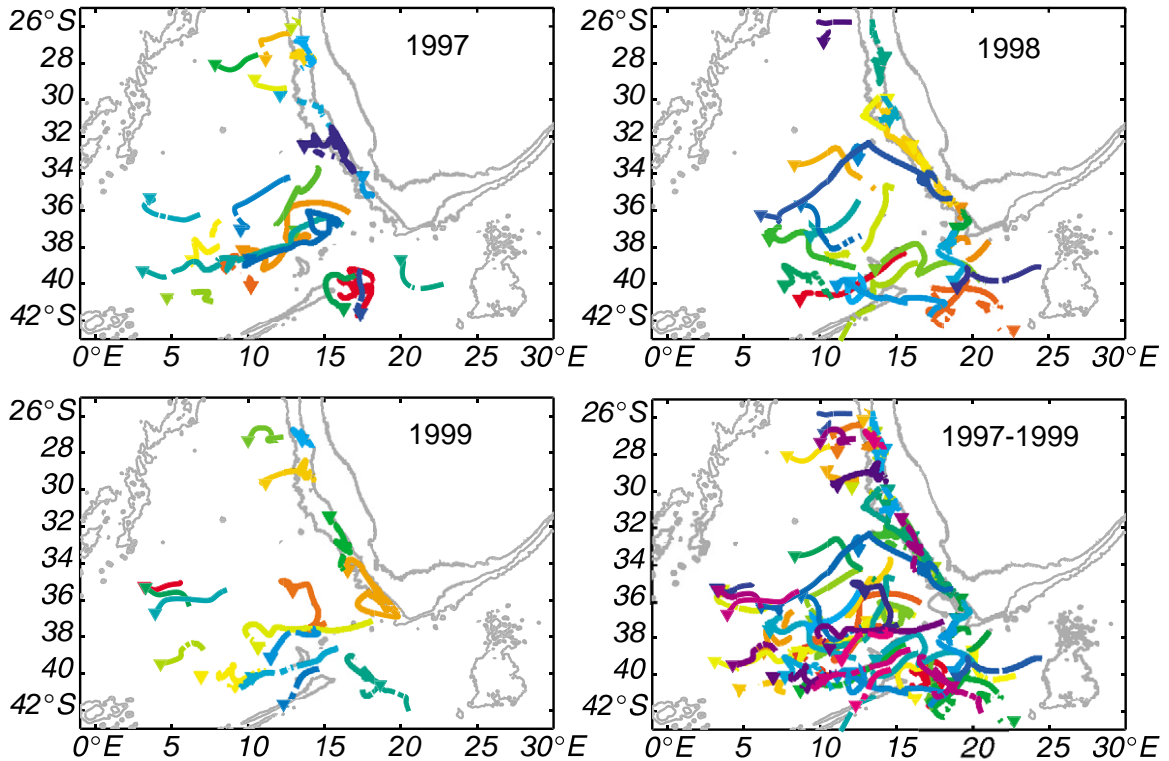


Fig. 6. Trajectories of cyclones in the Cape Cauldron as estimated from MODAS-2D SSH for the years 1997–1999 individually and accumulatively. Isobaths as in Fig. 1. Eddy trajectories end at the triangle.

subjective interpretation of Figs. 4, 7 and 8, we consider the “Cape Cauldron” as the geographical region delimited by the rectangle depicted in figures throughout this publication, with nodes at (31°S 15°E); (35°S 8°E); (41°S 13°E); and (37°S 20°E). Within the Cape Cauldron, surface MKE averages to  $5 \text{ J m}^{-3}$  and EKE to  $54 \text{ J m}^{-3}$ , while  $1 \text{ J m}^{-3}$  (MKE) and  $25 \text{ J m}^{-3}$  (EKE) apply to the intermediate layer (Table 1, column labeled “All”).

The observed values of intermediate depth Lagrangian kinetic energy fall in line with results from current meter moorings presented by Schmitz (1996). He reports on two moorings (838 and 834) to exhibit EKE of  $428$  and  $356 \text{ cm}^2 \text{ s}^{-2}$  at  $700 \text{ m}$  depth, and of  $201$  and  $149 \text{ cm}^2 \text{ s}^{-2}$  at  $1500 \text{ m}$ . These and our EKE levels are judged as consistent, given the fact that the current meters are above and below our average float depth and located at the southeastern boundary of the Cape Basin, where

EKE densities are expected to be the highest. Closer to the surface, at  $195 \text{ m}$  depth, only mooring 838 measured velocity, with an EKE of  $1347 \text{ cm}^2 \text{ s}^{-2}$ , comparable to the values found from MODAS in this region.

Schmitz (1996) noted that the observed EKE values from moorings are comparable to other energetic regions of the world oceans. However, in these other regions, the high EKE is dominated by the meandering of intense currents, such as the Gulf Stream or Kuroshio, and directly coupled to a strong mean flow, while in the Cape Cauldron this high MKE is missing. Past studies explained the enhanced EKE of the southeastern Cape Basin by passing Agulhas Rings within the otherwise uniform Benguela Drift. We suggest here that the regime of anticyclonic dominance is pushed past the boundaries of the Cape Cauldron, towards, and west of the Walvis Ridge. Within the Cape Cauldron, cyclones contribute at an even, if not

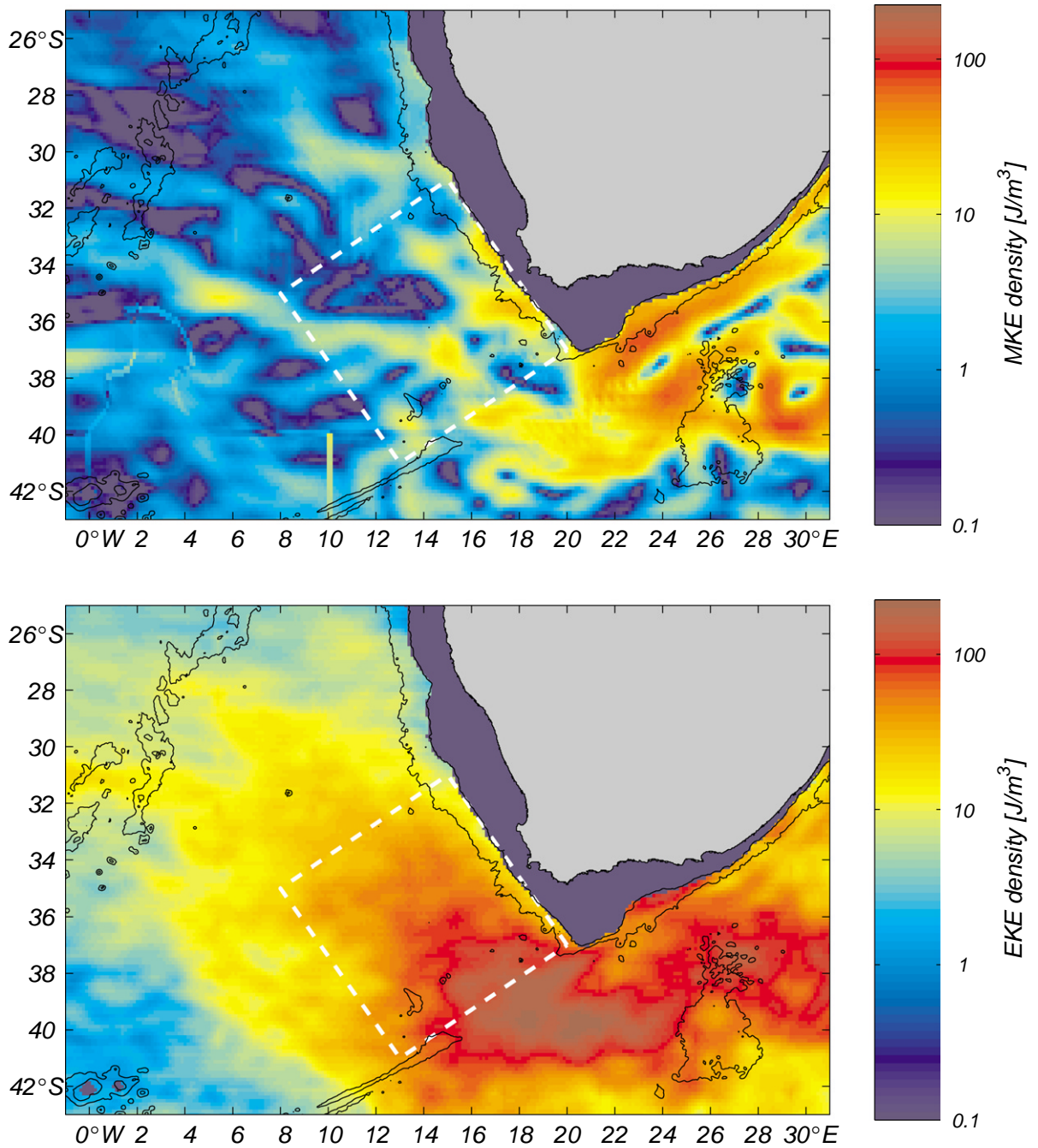


Fig. 7. Eulerian mean kinetic energy density (MKE, top) and eddy kinetic energy density (EKE, bottom) in the vicinity of the Cape Cauldron from MODAS-2D SSH data. Isobaths as in Fig. 1. The dashed white box indicates the Cape Cauldron.

Table 1  
MODAS-2D derived (top) and RAFOS float (bottom) velocity and energy estimates averaged over the “Cape Cauldron”

Selection	All	Cyclones	Anticyclones
Near surface (from MODAS-2D geostrophic estimates) from MODAS fields			
Number of data	4,359,590 (100%)	1,933,065 (44%)	2,087,696 (48%)
NdF	1084	481	519
$u$ (cm s <sup>-1</sup> )	0.2 ± 0.3	0.4 ± 0.5	0.1 ± 0.5
$v$ (cm s <sup>-1</sup> )	1.0 ± 0.2	0.7 ± 0.4	1.0 ± 0.4
MKE (J m <sup>-3</sup> )	4.5 ± 0.2	5.2 ± 0.3	5.4 ± 0.4
EKE (J m <sup>-3</sup> )	54.0 ± 1.4	56.2 ± 2.2	52.9 ± 2.0
TKE (J m <sup>-3</sup> )	58.5 ± 1.4	60.4 ± 2.2	57.4 ± 2.1
Intermediate depth (from RAFOS float data)			
Number of float days	2717 (100%)	1351 (49%)	873 (32%)
NdF	272	135	87
$u$ (cm s <sup>-1</sup> )	-0.9 ± 1.4	-1.2 ± 2.1	-0.6 ± 2.0
$v$ (cm s <sup>-1</sup> )	-1.0 ± 1.4	-0.8 ± 2.1	0.2 ± 2.1
MKE (J m <sup>-3</sup> )	0.9 ± 1.8	1.1 ± 4.5	0.2 ± 4.1
EKE (J m <sup>-3</sup> )	25.1 ± 2.6	30.5 ± 4.3	18.0 ± 3.5
TKE (J m <sup>-3</sup> )	25.2 ± 2.6	30.4 ± 4.3	18.1 ± 3.4

RAFOS float data were separated into cyclonic and anticyclonic subsamples according to the associated curvature vorticity exceeding  $0.5 \times 10^{-6} \text{ s}^{-1}$ . Error estimates for RAFOS float data are based on an effective number of degrees of freedom (NdF) calculated from the number of float days, while assuming an integral time scale of 10 days and simultaneous float velocity measurements by different floats to be independent. MODAS data were separated into cyclones and anticyclones according to the associated relative vorticity exceeding  $0.5 \times 10^{-6} \text{ s}^{-1}$ . Error estimates for MODAS derived quantities are based on the assumption of a 100 km spatial decorrelation radius and 10 days integral time scale. Rows indicate zonal ( $u$ ) and meridional ( $v$ ) velocity components, as well as mean, eddy, and total kinetic energy (MKE, EKE and TKE, respectively).

enhanced level to the variability, as the following section will show by separating the constituents of the enhanced EKE field into anticyclones and cyclones, using the feature recognition described in the section “2 Data and data processing”.

## 4. Cyclones and anticyclones

### 4.1. Anticyclones

Fig. 5 shows three annual and one cumulative panel of anticyclonic SSH derived eddy tracks. Please note that the annual panels show tracks of eddies that commenced in the year given, but which may extend into the following year(s), except for the 1999 panel, where trajectories are truncated on 31 December. SSH anticyclones are generally first recognized to the southwest of the Agulhas Bank by the tracking routine. The anticyclones enter the Cape Cauldron through a corridor formed by the deep channel between the

Agulhas Ridge and the Agulhas Bank (Fig. 1). Subsequent trajectories are located within the polygon spanned between this gap, 28°S 5°E and 34°S 0°E, i.e. the band described by Garzoli and Gordon (1996) as “Agulhas eddy corridor”.<sup>5</sup> None of our Rings chose a northern path, i.e. to cross 10°E north of 30°S, though two Rings each year passed over or north of Vema Seamount. While participating in an overall northwestward drift within the Cape Basin, details of the Ring’s drift appear quite erratic, particularly in the Cape Cauldron. For this region specifically, the average drift velocities of these anticyclones is to the northwest (Table 2), resulting in an average speed of  $3.8 \pm 1.2 \text{ cm s}^{-1}$ . The advection of the rings and their internal circulation becomes more

<sup>5</sup>It should be noted that the “Agulhas eddy corridor” is a somewhat ambivalent term, since any eddy shed by the greater Agulhas system is considered an Agulhas eddy, whereas the trajectories Garzoli and Gordon (1996) refer to are those of Agulhas Rings.

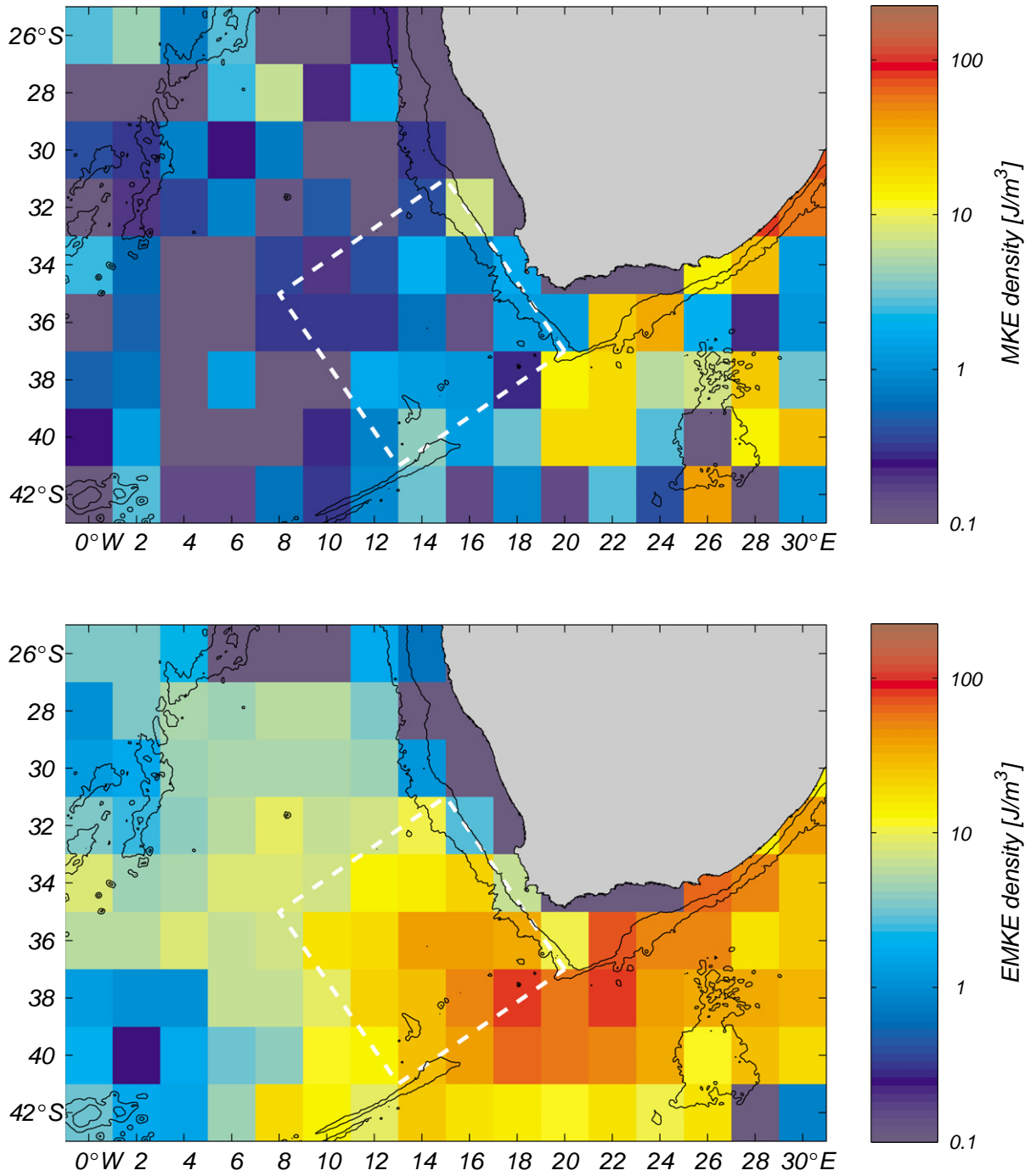


Fig. 8. Lagrangian MKE density and EKE density from RAFOS floats in  $2^\circ \times 2^\circ$  boxes. A dashed white box indicates the Cape Cauldron region. Isobaths as in Fig. 1.

Table 2  
Average kinematic properties of cyclonic and anticyclonic features within the Cape Cauldron as detected by MODAS-2D and RAFOS floats

Feature	Cyclones	Anticyclones
MODAS-2D derived features		
Number of features	43	29
$u$ (cm s <sup>-1</sup> )	-3.6±0.6	-3.6±1.0
$v$ (cm s <sup>-1</sup> )	-0.4±0.5	1.3±0.7
Ratio of no. of features	≈3:2	
RAFOS trajectory segments (all floats)		
Number of features	23	12
$u$ (cm s <sup>-1</sup> )	-1.8±2.8	-1.0±1.4
$v$ (cm s <sup>-1</sup> )	-3.0±5.8	3.0±5.0
Ratio of no. of features	≈2:1	
RAFOS trajectory segments (Cape Basin floats only)		
Number of features	17	11
$u$ (cm s <sup>-1</sup> )	-0.7±3.2	-0.9±1.6
$v$ (cm s <sup>-1</sup> )	-3.1±2.5	2.9±5.8
Ratio of no. of features	≈3:2	

Error estimates use the number of detected features as number of degrees of freedom and follow the routine described by Ollitrault (1994). Rows indicate zonal ( $u$ ) and meridional ( $v$ ) velocity components. Geostrophic MODAS surface velocity estimates are based on a continuous and complete coverage from 1 January 1997–31 December 1999. Subsurface RAFOS float data between 650 and 1150 m depth provide a nonuniform coverage of the period from March 1997–20 November 1998, when the last float exited the Cape Cauldron. The middle panel contains all floats, while the bottom panel includes only those floats launched in the Cape Basin.

monotonous when approaching the Walvis Ridge in which proximity they are deflected towards a more zonal (westward) direction, a motion also observed in numerical models (e.g., Matano and Beier, 2003 or Treguier et al., 2003). In the northwestern Cape Basin, where the energy levels are significantly lower, Agulhas Rings are observed to assume their well-known circular shape.

The number of anticyclones observed in the Cape Cauldron is 14 in 1997, 8 in 1998 and 7 in 1999. These numbers are significantly higher than the number of anticyclones observed to cross 5°E (outside the Cape Cauldron) in 1997, 1998 and 1999, which are 3, 3 and 4, respectively. This later estimate is based on a modified requirement of each track's duration surpassing 4 months, intending to capture those eddies that most likely

represent longer lived Agulhas Rings, which continue across the Walvis and Mid-Atlantic Ridge (Treguier et al., 2003). Earlier findings of Garzoli and Gordon (1996) corroborate the observed decrease in number of rings with increasing distance from the Retroflexion.

The number of anticyclones observed here should be considered as a lower limit, since modifications of the detection parameters produce somewhat higher values (+1 or 2). The difficulty stems from undetected differences between the actual and an assumed mean seasonal steric heaving of sea surface, which is subtracted from the SSH signal. Another unknown lies in the spatial variability of the climatological fields that enter the calculation of absolute SSH. The higher numbers of trajectories reported to commence in 1997 might partially be due to trajectories that originated in 1996 or earlier, but which fall into the 1997 category due to our SSH data set beginning on 1 January 1997. In analogy, trajectories beginning in 1999 might be truncated by the termination of the SSH data on 31 December 1999.

The majority of anticyclones observed had lifetimes of around 100 days, significantly above the minimum detection requirement of 60 days. However, relative to the order of years lifetimes of mature Agulhas Rings, the observed average lifetime of anticyclones in the Cape Basin is low. This is a repercussion of the strong variability in this region. Variations in strength due to the seasonal steric SSH variation as well as repeated splitting and merging of eddies or rapid displacements (Schmid et al., 2003), make it very difficult to assign SSH anomalies to a single mesoscale feature over an extended period of time.

These results for the sea-surface from MODAS-2D SSH are confirmed by RAFOS float observations (Fig. 3) at intermediate depth. Anticyclonic float trajectories that feature several revolutions are most prominent to the northwest of the Cape Cauldron. Further anticyclonic motion is noticeable along the offshore/anticyclonic side of the Agulhas Current and within the first meander crest of the Agulhas Return Current (Boebel et al., 2003). Some anticyclonic trajectory segments are observed to the southwest of the Cape Cauldron, where anticyclones from the Brazil–Malvinas

Confluence Zone could enter the area of interest. However, all but one of these segments depicts an overall southward component, counter to the expected northward direction.

Within the Cape Cauldron only 4 out of 9 features follow the anticipated north to northwestward route (Fig. 3, top right panel). While the mean flow sets in a northwestward direction, the associated error, calculated from the variability between eddy displacements, renders it insignificantly different from zero (Table 2). The mean particle (i.e. float) speed within these features and the Cape Cauldron averages to  $15.9 \pm 5.1 \text{ cm s}^{-1}$  at intermediate depth. Visual estimates of typical eddy diameters from these anticyclonic RAFOS float trajectory segments vary around 200 km.

A number of past publications, due to the observation of colder thermostads and high oxygen values near saturation (Garzoli et al., 1999), provided controversial opinions on the possibility of entrainment of Brazil Current Rings into the Cape Basin. Some studies (Duncombe Rae et al., 1996) suggest that, after having been swept across the Atlantic with the South Atlantic Current, the rings enter the Benguela Current from either the west, or the east after having been entrained into the South-West Indian Recirculation. While in our data no anticyclone enters the Cape Cauldron from the southwest, entrainment from the southeastern subantarctic region cannot be excluded. However, the high variability observed in the Cape Cauldron as documented herein, combined with the long residence time of water in this region, suggests that extensive isopycnal and diapycnal mixing events can occur (Schmid et al., 2003). Therefore it is possible that the observed anomalies are locally modified water of Agulhas Current origin.

The modification of water mass characteristics within the anticyclones appears also likely from numerous observations of ring merging, splitting and deformation. The complementary movie suggests that Agulhas Rings reconnect to the Agulhas Retroflection proper on 7 occasions in 3 years, with one of these events being documented in the set of snapshots given by Schmid et al. (2003). The most extreme event bridged the distance from the Agulhas Retroflection to a ring

at 35°S, i.e. order of 600 km, providing a fast track for undiluted Agulhas Water to enter far into the Cape Cauldron.

#### 4.2. Cyclones

MODAS-2D SSH depicts most cyclones to be limited in their existence to the Cape Cauldron region. In 1997, 22 such cyclones were observed in total, some of which might have already been formed in 1996. In 1998 the detection scheme revealed 24 cyclones, and 16 cyclones in 1999. Within the Cape Cauldron their drift exhibits an overall west-southwestward trend. The mean zonal velocity is  $-3.6 \pm 0.6 \text{ cm s}^{-1}$  and the mean meridional component  $-0.4 \pm 0.5 \text{ cm s}^{-1}$  (Table 2).

The cyclones' lifetimes tend to be shorter than those of anticyclones, with the majority having only 2–3 months duration. This value however, is right at the lower limit requested by the eddy recognition routine, and thus, since shorter lifetimes are filtered out, the true mean could be lower than the estimate given. Scrutiny of Fig. 6 suggests that the SSH cyclones found in the Cape Cauldron are formed in three distinctly different locations.

- (1) *Agulhas cyclones* (Lutjeharms et al., 2003), formed inshore of the Agulhas current. This variety consists of the well-known Natal Pulse and a close cousin thereof, i.e. a pulse formed near Port Elizabeth rather than in the Natal Bight. (See the movie `the_cape_cauldron_agulhas_cyclone.avi` for an illustration of such an event.) These pulses carry Indian Ocean water. Since isopycnals shoal by some 300–500 m within the cyclone embedded in the pulse, these eddies do not contain the lightest variety of Agulhas waters. A third relative of these cyclones is found to form at the tip of the Agulhas Bank, where the Agulhas Current detaches from the topography. Here, a cyclonic circulation is shown repeatedly in various data sets (Penven et al., 2001). The water entrained into this particular cyclone is likely to be supplied by the cyclonic side of the Agulhas Current.
- (2) *Subantarctic cyclones*, formed in the subantarctic zone, primarily due south of Cape

Agulhas. These cyclones are expected to carry water of subantarctic properties. It is noteworthy though, that no subantarctic cyclones are formed west of the Agulhas Retroflexion. In fact, all such cyclones pass through the same gap as the Agulhas Rings, i.e. the deep channel between the tip of the Agulhas Bank and the Agulhas Ridge, having originated farther to the southeast. (See the movie *the\_cape\_cauldron\_subantarctic\_cyclone.avi* for an illustration of such an event.)

- (3) *Cape Basin cyclones*, formed along the western shelf break of southern Africa. These cyclones probably contain water of any mixture to be observed in the Cape Basin since they form locally. (See the movie *the\_cape\_cauldron\_upwelling\_cyclone.avi* for an illustration of such an event.) Their formation could be related to the interaction of Agulhas Rings with the shelf, to the local upwelling along the East African shelf (Shannon and Nelson, 1996) or to an intermediate eastern boundary current, which is suggested to emerge out of the Angola Basin to flow poleward along the African shelf break (Shannon and Hunter, 1988).

These views of the sea-surface are supported by the location of cyclonic RAFOS float trajectory segments (Fig. 3) within the intermediate depth horizon. Cyclonic float trajectory segments commence from all 3 formation regions. However, while RAFOS floats depict Agulhas cyclones entering the Cape Cauldron, no such event is documented by floats for subantarctic cyclones (in contrast but not in contradiction to the SSH results). The (float) cyclones formed near South Africa's west coast predominantly drift southwestward. The ensemble mean of cyclonic motion in the Cape Cauldron averages to  $3.5 \text{ cm s}^{-1}$  speed in west-southwestward directions, though large errors associated with these values (Table 2) render this mean not significantly different from zero. The mean float speed within these features averages to  $21.9 \pm 3.0 \text{ cm s}^{-1}$ . The mean duration of these trajectory segments is 40 days (within the Cape Cauldron), with a nearly uniform distribution reaching up to 2 months. While some trajectories

are surpassing this value after leaving the Cape Cauldron to the southwest, both, MODAS and RAFOS results agree in suggesting a typical 2–3 months lifetime of these cyclones. Visual estimates of cyclonic RAFOS float trajectories loops suggest a representative diameter of 120 km.

Our observations differ substantially from previous suggestions that only a few cyclones exist in the Cape Basin. While cyclones have been observed both in in-situ data (Duncombe Rae et al., 1996) and through satellite measurements (Gründlingh, 1995, 1999), their importance was diminished on the basis of their short lifetime (<3 month). As discussed below, it is the different evaluation of their role with regard to stirring and mixing the Indian Ocean inflow, particularly at intermediate depth, that distinguishes our interpretation from the previous ones.

A second important point needs mentioning. Previous descriptions of cyclones in the Cape Basin suggested they contain cores of subantarctic waters due to their formation process, i.e. the northward wedging of subantarctic water when an Agulhas Ring is shed (Lutjeharms and Gordon, 1987). The combined RAFOS/MODAS observations suggest that cyclones may as well be of subtropical origin, carrying waters intrinsic to the Agulhas or the Cape Basin. While doming isopycnals within these features create a cold surface signal, in resemblance of water from the subantarctic region, TS diagrams, particularly at intermediate depth would reveal their true origin. Unfortunately such data is currently unavailable but might soon be revealed within the Dutch Mixing of Agulhas Ring Experiment (MARE) (van Aken et al., 2003).

#### 4.3. Cyclone/anticyclone comparison and interaction

Probably the most important finding made so far is the recognition that cyclones occur at a significant rate within the Cape Cauldron. The ratio between cyclones and anticyclones is near 3:2 in favor of cyclones. Subsurface features captured by floats are generally also visible at the sea-surface in the MODAS data, i.e. all features identified at intermediate depth extend up to the

surface. Whether all MODAS surface features extend down to intermediate depth is difficult to say, due to the inhomogeneous spatial/temporal coverage of the floats. However, we could not identify significant mismatches between the RAFOS and MODAS patterns of motion in the Cape Cauldron. It is hence conjectured that the ratio of surface to intermediate depth features is insignificantly different from 1, for both cyclones and anticyclones. The absolute mean phase speed of both groups is similar, between 3 and 4 cm s<sup>-1</sup>. The total time spent by floats in anticyclones (523 days) is lower than the time spent in cyclones (949 days), with a ratio (0.55).

Of no lesser importance is that in both SSH and RAFOS data, cyclones and anticyclones depict differential drift patterns. While most anticyclones drift in a northwestward direction, most cyclones follow west–southwestward routes. Both trends are expected for nonlinear eddies on a  $\beta$ -plane (Flierl, 1981). While the SSH derived results show significant means, the means from the RAFOS float derived eddy displacements differ insignificantly from stagnation, based on their associated 95% confidence intervals.

A greater density of cyclonic over anticyclonic data is noticeable in the Cape Cauldron, especially in the trajectories (Table 2, middle panel). It cannot be excluded that this asymmetry is due to the initial setting of floats, which, at least for the floats deployed directly into the Agulhas Current (Lutjeharms et al., 2003), were heavily biased towards the cyclonic side of the current. While 6 cyclonic trajectory segments resulted from floats launched into the AC, only 1 AC float depicted an anticyclonic pattern within the Cape Cauldron. In contrast, the floats set into the Cape Basin during the R.V. *Polarstern* cruise ANT XIV, were launched in a more regular pattern along the cruise track. Therefore, the launch positions of these 30 floats are unbiased towards a specific oceanographic environment, with the exception of 5 floats, which were explicitly launched into an anticyclonic Agulhas Ring (Schmid et al., 2003). For this group of Cape Basin floats, the ratio of float segments showing cyclonic and anticyclonic motion is 17:11 (Table 2, bottom panel), i.e. nearly identical with the 43:29 ratio observed in the MODAS data.

Similar float trapping times by individual cyclones (44 days) and anticyclones (41 days) are suggested when calculating the ratios between total time spent within such features and the number of features observed. The tangential speeds as approximated by the RAFOS floats, were higher within the cyclones ( $21.9 \pm 3.0$  cm s<sup>-1</sup>) than within anticyclones ( $15.9 \pm 5.1$  cm s<sup>-1</sup>). This finding is corroborated by the overall statistical analysis of RAFOS data discussed in the section “Defining the Cape Cauldron” and presented in Table 1. Cyclones and anticyclones show at intermediate depth significantly different levels of Lagrangian eddy kinetic energy densities (EKE). The cyclonic eddies exhibit energy levels that are elevated by 60% over those of the anticyclones. However, similar calculations for the MODAS derived velocity fields show no such difference near the surface (Table 1) for the Eulerian EKE.

Modeling results of Matano and Beier (2003) suggest a subsurface intensification of cyclones in this region. In their model, cyclones and anticyclones are paired in form of hetons (Hogg and Stommel, 1985). The high eddy density in the Cape Cauldron, however, makes it difficult to maintain an extended association of a given cyclone/anticyclone pair, particularly since the cyclones and anticyclones appear to have different mean drifts. It is also questionable if the increased kinetic energy levels observed by the floats reflect a higher cyclonic intensity, or if they are only a consequence of the kinematic amplification due to the different sign of the centrifugal term in the gradient wind equation.

The joint animation of MODAS and RAFOS data (see movie *the\_cape\_cauldron\_ssh.avi*) suggests that at any given moment several anticyclones and cyclones are coexistent in the Cape Cauldron. The floats’ frequent change between anticyclonic and cyclonic segments is judged as evidence of the entrainment and detrainment of water into the various features, and consequently of the thorough stirring of waters temporarily trapped within these features. Agulhas Rings have been observed to be displaced at speeds up to 27 cm s<sup>-1</sup> (Schmid et al., 2003), which is comparable to their internal tangential speed at intermediate depth (the mean float speed averages at

$16 \text{ cm s}^{-1}$ , see Section 4.1. Anticyclones”). Based on the suggestions made by Flierl (1981), it is therefore conjectured that Agulhas Rings can lose substantial amounts of the intermediate water within the Cape Cauldron. The reverse effect, i.e. the entrainment of Benguela upwelling water by passing Agulhas Ring, has been documented previously by Duncombe Rae et al. (1992).

The cyclones, however, do not only participate in the inter-ocean exchange through facilitating the mixing of Agulhas Waters into the Cape Basin background. They also seem to be instrumental in the cut-off process when Agulhas Rings are shed. For 16 Agulhas Ring spawning events that could clearly be identified between 1997 and 1999, half (8) were related to the northward protrusion of subantarctic water, 5 directly related to an Agulhas cyclone breaking through the Retroflexion to the south, and 3 more were linked to the southward migration of a cyclone that appeared to have formed locally at the Agulhas Plateau. While the southward moving Agulhas cyclones appear to initialize the Agulhas Retroflexion cut-off process in a causative sense, the causality remains unclear for the northward propagating subantarctic cyclones.

## 5. Inter-ocean exchange

### 5.1. Pathways

How does the joint action of anticyclones and cyclones facilitate the inter-ocean exchange at intermediate depth? Let us set aside the separation between cyclones and anticyclones and take an inherently Lagrangian view. Fig. 9 shows a set of panels depicting only those float trajectories that enter a predefined box during their lifetime. Trajectories shown represent the time span between the floats’ setting and the moment they enter the box. Borrowing from the meteorological terminology, we call these plots hindcasts hereinafter. These form an important analytical tool to establish the origins of waters found at a given location and have previously been used in ocean models to successfully illustrate and quantify the large-scale circulation (Döös, 1995). In Fig. 10

forecasts, i.e. trajectories of floats emerging from a certain box are shown in an analogous fashion, with trajectories ending at the time the float surfaced. Please note that trajectories might cover widely varying time spans.

The Cape Basin outflow across the Walvis Ridge (box centered at  $31^\circ\text{S}$ ,  $3^\circ\text{E}$ ) clearly derives its waters primarily from the east (Fig. 9a) and interior Cape Basin and releases them to the west (Fig. 10a). A detailed analysis of the flow field provided by Richardson and Garzoli (2003) suggests a predominantly zonal mean flow at intermediate depth in this region. Located in the middle of the contributory region of this inflow box, a second box in the central Cape Basin at  $33.5^\circ\text{S}$ ,  $8.5^\circ\text{E}$  is fed (Fig. 9b) by waters from all directions, but releases floats primarily to the northwest (Fig. 10b).

The next pair of panels (c) depicts trajectories intersecting a box centered in the Cape Cauldron at  $36^\circ\text{S}$ ,  $14^\circ\text{E}$ . Trajectories entering this box originated in the Agulhas Current, to the south of the Subtropical Convergence and near  $30^\circ\text{S}$  (Fig. 9c), giving an impression of the diversity of water masses that are likely to enter this box.<sup>6</sup> A quasi-isotropic distribution of trajectories emerges from this box (Fig. 10c). The trajectory field appears to be dominated by cyclonic motion within the Cape Cauldron, with several trajectories feeding into the Agulhas Return Current, indicative of an Atlantic to Indian exchange.

The concept of a bi-directional exchange is corroborated by trajectories entering and emerging from a box located at the tip of the Agulhas Bank at  $38.5^\circ\text{S}$ ,  $19.5^\circ\text{E}$ . The box is supplied with water from the Agulhas Current, but also from the sector to the west of it (Fig. 9d). The only sector not feeding into this box is located to its southeast, where the Agulhas Return Current (ARC) emerges out of the box (Fig. 10d). The ARC forms the main drainage of this box, but water is also

<sup>6</sup>It should be noted that float trajectories are not an unambiguous proof that a parcel of water has taken the same route. Isobaric floats in particular will separate from the water parcel they tag when the parcel is vertically displaced. Isopycnal floats will deviate to a significantly lesser extent.

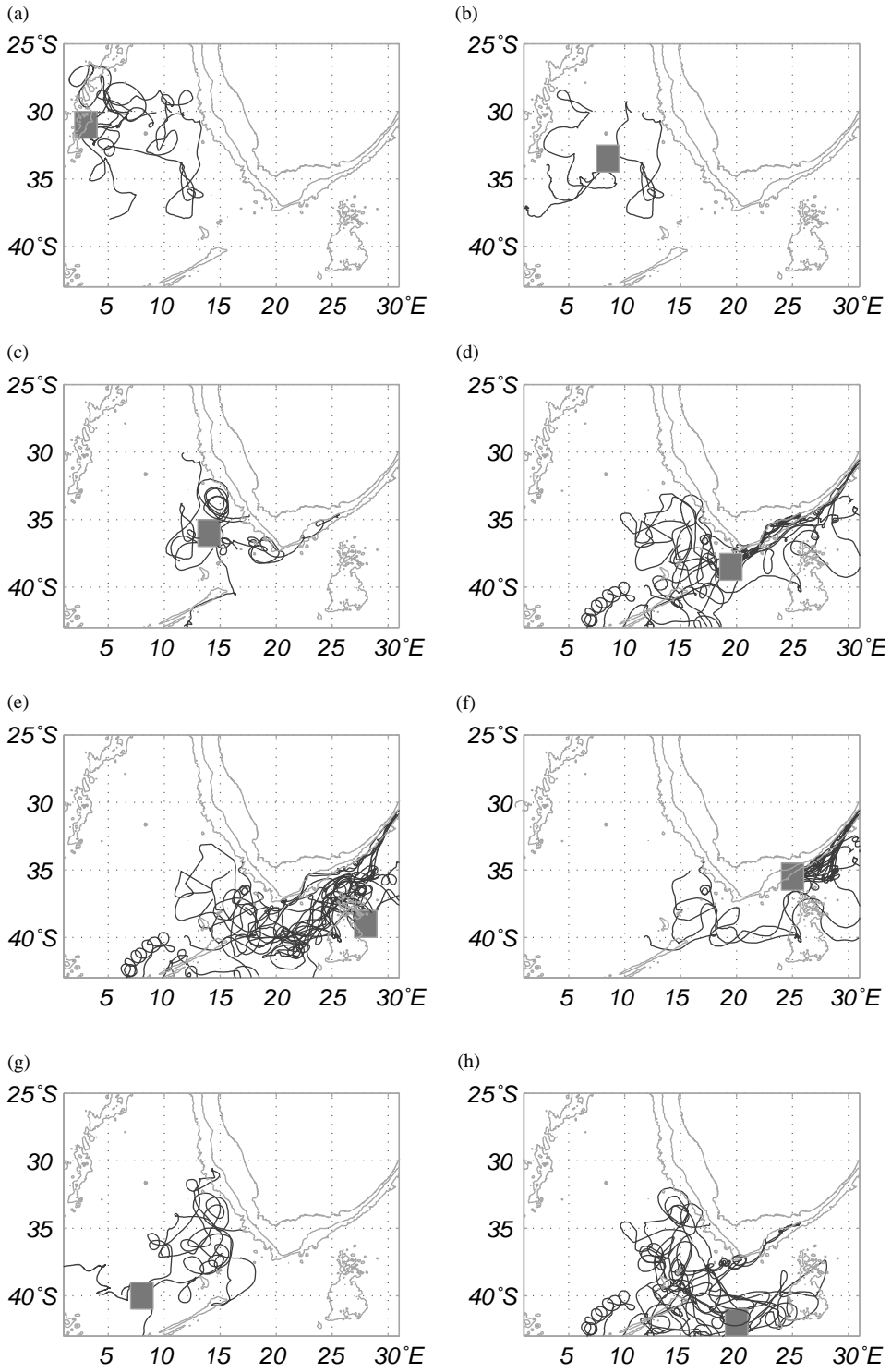


Fig. 9. Hindcasts of RAFOS float trajectories that transect the indicated boxes during their mission.

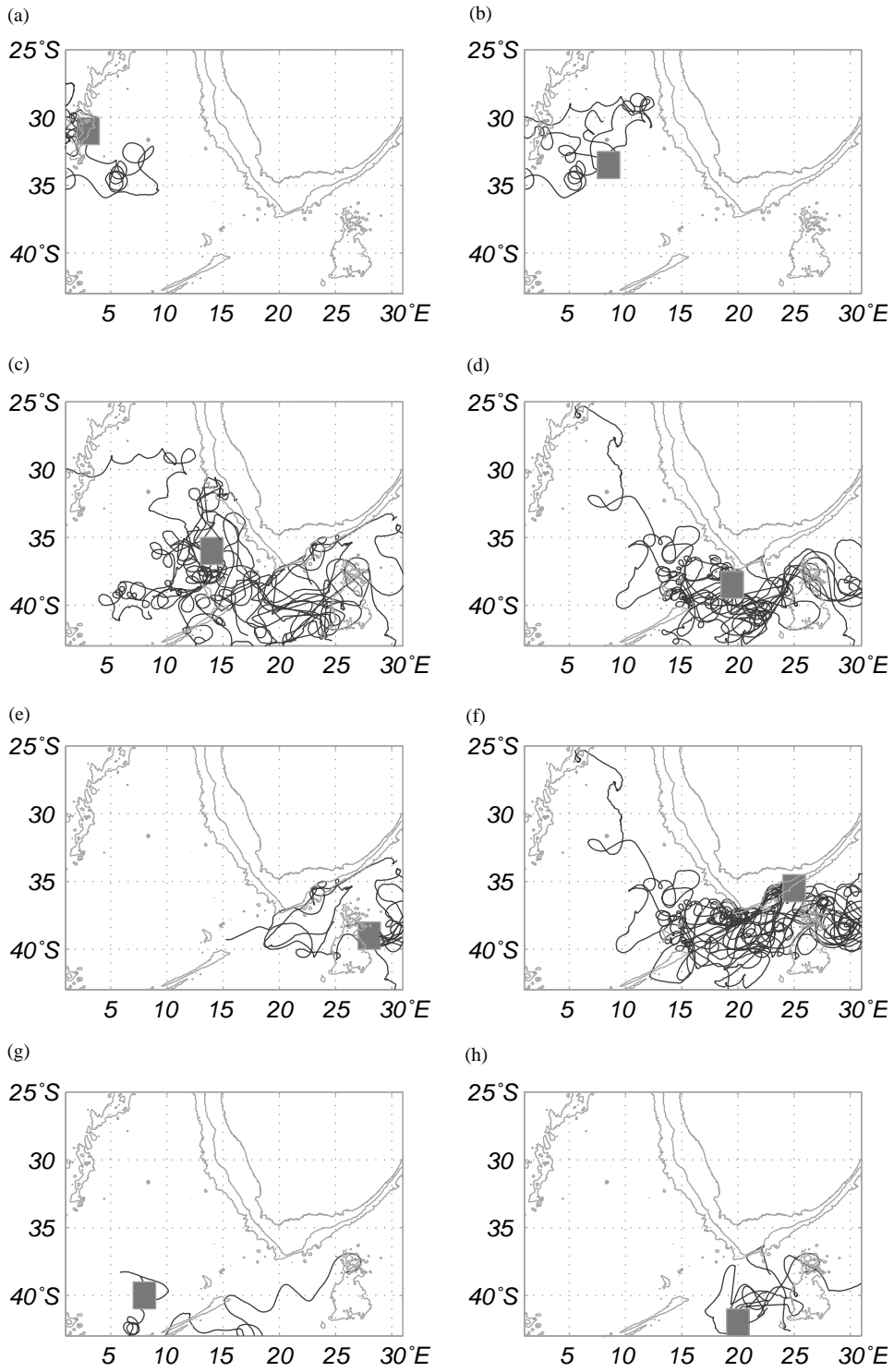


Fig. 10. Forecasts of RAFOS float trajectories that transect the indicated boxes during their mission.

expelled into the Cape Cauldron, where again cyclonically looping trajectories are dominant.

The tributaries to the Agulhas Return Current are captured in (Fig. 9e). The box, centered at 39°S, 28°E, is located right across the path of the ARC after it circumnavigated the Agulhas Plateau. This meander has been shown to be topographically trapped and to be quasi-permanent (Boebel et al., 2003), which is reflected by the large number of trajectories that enter this box from the northwest (exclusively!). The trajectories originate in the Agulhas Current proper, the Cape Cauldron and in the vicinity of the nominal position of the Subtropical Convergence. Trajectories exiting this box (Fig. 10e) escape to the southeast, primarily with the ARC, with one trajectory depicting a full local recirculation in the Agulhas Current/Agulhas Return Current system.

Fig. 9f finally shows trajectories that pass through the southern Agulhas Current. Due to a large number of floats launched upstream of this box (36.5°S, 25°E) and explicitly into the Agulhas Current, the figure is dominated by trajectories entering the box from the northeast. However, 2 trajectories, emerging from the Cape Cauldron, enter the AC via the above mentioned local recirculation gyre, showing the possible influence of modified water of Atlantic origin on the AC. The outflow (Fig. 10f) is not unexpectedly solely to the southwest with the AC, feeding primarily into the Agulhas Return Current and the Cape Cauldron.

Combining these different panels, one could easily construct a pathway from the Agulhas Current (box f) to the Benguela Drift regime (box a). It is well known, however, that the Benguela Drift water mass properties are not identical with those of the Agulhas Current. To provide the lower salinities (with respect to the AC salinities) of the Benguela outflow, a second source of Atlantic origin is necessary. The region that has been considered in the past to provide such input lies to the southwest of the Cape Cauldron and is exemplified here by the box at 40°S, 8°E in (Fig. 9g) and (Fig. 10g). However, the resulting selection of trajectories suggests this region to be fed by water from the Cape Cauldron, and to

release its water into the Subantarctic Zone adjacent to the ARC rather than vice-versa as anticipated. Similar to box “g”, a surprising flow is associated with the 42°S, 20°E box “h” due south of the tip of the Agulhas Bank and mostly on the cyclonic side of the Agulhas Retroflexion (Figs. 9h and 10h). Fed by water from the Cape Cauldron, the Subantarctic Zone west of the box and the AC, water from the box remains mostly south of the ARC and does not enter the Cape Cauldron directly.

These findings amplify Gordon et al.’s (1992) suggestions of an indirect closure of the South Atlantic’s subtropical gyre. Their study analyzes the partitioning of the inflow by water mass analysis using the SAVE hydrographic and tracer sections. In their conclusion, South Atlantic water, rather than folding directly into the Benguela, enters the Indian Ocean loop and feeds indirectly into the Cape Basin via the Agulhas Leakage. 65% thermocline and 50% intermediate water are reportedly fed into Benguela Drift this way. The remaining volume is suggested to be injected from the South Atlantic into the Benguela Drift at western edge of Agulhas retroflexion, presumably during the frequent eddy shedding periods. Our findings suggest a dominance of the indirect route at intermediate depth, with only a small amount of inflow from the Atlantic directly.

Finally, one may ask why there is not a single continuous float trajectory from the Agulhas Current to the Mid-Atlantic Ridge? We think that such trajectories could exist, but that the floats’ maximum mission duration of 2 years was not sufficient to capture such a path. The high turbulence in the Cape Cauldron resulted in extended residence time for the floats there, so that the floats surfaced before they were able to reach across the MAR. In addition, care must be taken in the discussion of pathways. The number of floats launched in a specific region can significantly bias the distribution of trajectories and emphasize one tributary over others.

## 5.2. Transport estimates

Mean RAFOS float velocities averaged over partially overlapping  $3^\circ \times 3^\circ$  boxes on a  $1.5^\circ \times 1.5^\circ$

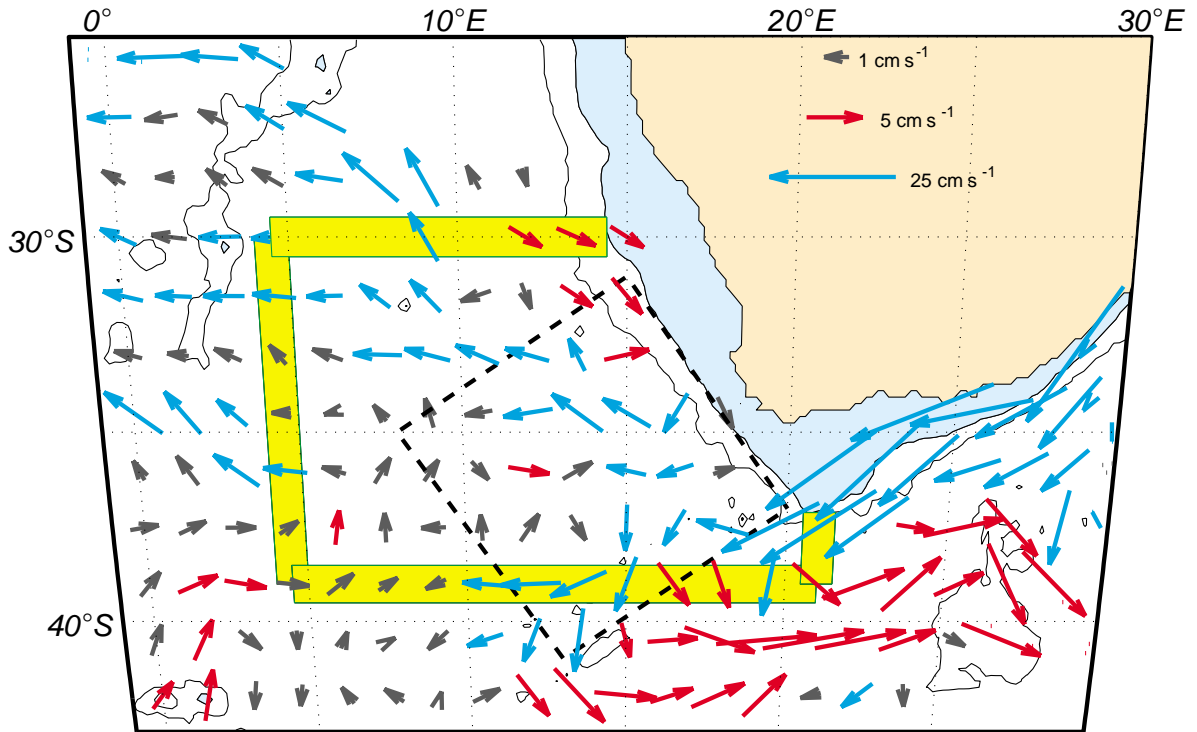


Fig. 11. Mean flow field at intermediate depth from RAFOS floats. Colored arrows indicate speed  $\geq 3 \text{ cm s}^{-1}$ , red if the zonal component is eastward, blue if westward. Black arrows if speed  $< 3 \text{ cm s}^{-1}$ . Note the nonlinear speed scale: arrow length is proportional to the square root of speed to accommodate a wide range of velocities.

grid provide the intermediate depth velocity field given in Fig. 11. Arrows are in color if float speeds exceed  $3 \text{ cm s}^{-1}$ , with red representing arrows that have an eastward zonal component, blue if westward. Arrow length indicates the square root of the mean speed to accommodate the high speeds in the Agulhas Current and the low speeds in the open ocean within the same plot. Southwestward velocities in the Agulhas Current and eastward flow in the Agulhas Return Current are palpable. The outflow region near the Walvis Ridge is dominated by northwestward flow to the east, and westward flow to the west of the Walvis Ridge. Farther east, shoreward of  $12^\circ\text{E}$ , some vectors even seem to indicate the suspected inflow of Antarctic Intermediate Water (AAIW) emerging from the tropical regime to the north (You, 2002).

Around  $40^\circ\text{S}$ , to the west of  $10^\circ\text{E}$ , where one would suspect the South Atlantic Current to come into view, a predominantly sluggish flow field is

observed, which has a slight northeastward tendency. Within the Cape Cauldron, increased velocities with a westward tendency emerge. The ‘mean’ Agulhas Current, entering obliquely into the southern part of the Cape Cauldron appears to bifurcate into two branches: a northern branch, which feeds into the outflow across the Walvis Ridge, and a southern branch, which commences to retroflect in the southern part of the Cape Cauldron, connecting to the eastward flowing ARC. From the previous discussion it is clear that such a “mean” view is inappropriate to describe this region’s kinematic, but it nevertheless serves well to describe the result of the intense stirring and mixing processes at intermediate depth.

Averaging float velocities within a given band along a virtual section can be used to establish crude estimates of intermediate depth transport. In close resemblance to the sections selected by Matano and Beier (2003), we estimate the

Table 3  
 RAFOS float data-based transports perpendicular to sections surrounding the Cape Cauldron

Section	Transport (Sv)	Ratio	Section limits	Section width (km)
East	$-32 \pm 15$	+ 100%	21°E; 37.1°–39.0°S	211
South	$-23 \pm 22$	–72%	39°S; 4.5°–21.0°E	1414
West	$-7 \pm 9$	–22%	4.5°E; 30.0°–39.0°S	1001
North	$+3.0 \pm 8$	–6%	30°S; 4.5°–14.4°E	958

Please see Fig. 11 for locations. Positive transports are north- or eastwards; negative transports point south- or westwards. The column “ratio” indicates the relative contribution of each section to a total flux of 100%. Negative ratios indicate outflow from the box, the positive value of 100% refers to the inflow with the AC. Estimates are based on all float data found between 650 and 1250 m depth within the polygons associated with each section. Standard errors assume a Lagrangian decorrelation time of 10 days.

inflowing transport across the eastern section, the outflow across the western and northern sections and the southern in/outflow (Table 3 and yellow bars in Fig. 11). The estimates are based on all float velocities within each “section” assuming a mean layer thickness of 600 m. The results are reasonable, with the Agulhas inflow amounting to  $32 \pm 15$  Sv, and the box residual being only 1 Sv (32 Sv in, 33 Sv out). Our results emphasize the AC as the main tributary to the Cape Cauldron with order of 9 Sv effective input at intermediate depth ( $23 \pm 22$  leave the box with the ARC). A total of  $7 \pm 9$  Sv leave the box to the east while  $3 \pm 8$  Sv cross the boundary to the north. Our results, and particularly their ratios (Table 3), compare well with those presented by Matano and Beier (2003). However, the RAFOS float based transport values are of the same order as their associated errors (estimated from the variance of the daily float velocities and assuming a 10-day Lagrangian time scale) and hence their meaningfulness is limited.

Based on the BEST hydrographic and IES data, Garzoli and Gordon (1996) estimated the 1.5 year mean transports relative to 1000 m into the source region of the Benguela (see their Fig. 7). From these transports they conclude that the Benguela Drift is composed of 50% South Atlantic water, 25% Indian Ocean (Agulhas) water and 25% blended tropical Atlantic and Indian Ocean waters. The assignment is based on the geometric location of the sections, with 3 Sv from a section located in the center of the Cape Cauldron assigned exclusively to the Agulhas inflow, 3 Sv from across the shelf to a mix of tropical Atlantic and Indian Ocean water, and 6 Sv inflow across

the western boundary of their area of study as Atlantic inflow. The difficulty of establishing mean transports in this highly energetic region is however immediately reflected in Garzoli and Gordon’s error estimates for these transport values: The associated standard deviation exceeds the mean by up to a factor of 2, except for the northward outflow across 30°S (10 Sv). The resulting schematic flow diagram from such hydrographic data is compromised by the fact that velocities can only be estimated perpendicular to a given section and hence provide only limited information on flow directions.

How do these results compare to our findings? Obviously inter-annual variation might have changed the in/outflow ratios between the BEST and KAPEX years, basically rendering it impossible to hold one result over the other. Furthermore, BEST describes intermediate and thermocline waters, while our transport estimates are for the intermediate layer only. However, the close match of MODAS and RAFOS mesoscale flow patterns suggests that the advection of mesoscale signals and hence their associated transports extend throughout at least the thermocline and intermediate horizons of the water column.

We therefore conclude that most of the water that feeds the northern, westward flowing limb of the subtropical gyre is funneled through the Cape Cauldron while very little is entrained directly from the region to the southwest of the Cape Cauldron, i.e. the nominal location of the SAC. It is feasible however, that water of this origin is entrained into the interior Cape Cauldron region

either during the formation of subantarctic cyclones during Agulhas Ring shedding events or into the interior Agulhas Recirculation region when eddies from the subantarctic zone are shed to the north from the Agulhas Return Current. These eddies have been shown to drift westward between the AC and ARC and to finally become entrained into the Retroflexion region, from where Atlantic AAIW can enter the Cape Cauldron.

Our transport estimates are larger than those based on the analysis of Agulhas Rings anomalies. Based on the concept presented here, using a reference station from the interior Atlantic east of the Cape Cauldron and a reference depth of 1600 m, Schmid et al.'s (2003) estimates result in transports of  $27 \times 10^{-3}$ – $40 \times 10^{-3}$  PW,  $48 \times 10^{12}$ – $60 \times 10^{12}$  kg salt and 5–8 Sv of water. The numbers given span the typical of 4–6 Agulhas rings per year and are based on the combined analysis of KAPEX hydrographic and RAFOS float data for a juvenile (age <6 months since spawning) Agulhas Ring. These estimates are at the high end or exceed those given in other studies (Duncombe Rae et al., 1996), which is to be expected,<sup>7</sup> but are still significantly smaller than the results given herein, which provide 9–10 Sv inflow for the intermediate level only. However, allowing for order of 6–10 rings per year to enter the Cape Cauldron, within which some of the rings would dissipate and release their anomalies as implied by our results, one could accommodate the missing amount.

## 6. Summary and outlook

It is the intent of this paper to draw the reader's attention to the role played by the cyclones, their interaction with the Agulhas Rings (in the Cape Cauldron), and their impact on the inter-ocean exchange. We showed that high EKE at both the surface and intermediate depth exist in the Cape Cauldron, a tell-tale signature of eddy induced stirring processes. Subsequently, we demonstrated

that this field of enhanced eddy kinetic energy is composed of differentially moving cyclonic and anticyclonic vortices; some of them are of Indian Ocean descent while others enter from the subantarctic regime or develop locally. From this we concluded that both Indian and Atlantic waters are injected into the Cape Cauldron, not only at the surface but also at intermediate depth. As can be seen in the supplemental movie or the set of snapshots given by Schmid et al. (2003), the vortices, while in the Cape Cauldron, undergo significant deformations and floats exchange freely between anticyclonic and cyclonic eddies. This, together with the hydrographic evidence presented by Schmid et al. (2003) supports the conjecture that the Indian and Atlantic types of AAIW are not only stirred but also thoroughly mixed in the Cape Cauldron. Our float trajectories suggest a small direct inflow of fresh AAIW from the west, while suggesting bi-directional exchange between the Atlantic and Indian Oceans. Transports calculated from average float velocities across selected sections quantify the inter-ocean exchange and ensuing export to the Benguela Drift at about 10 Sv for the intermediate layer. While this result is compromised by a large formal error, it nevertheless is of the same magnitude as the independent estimate of  $15 \pm 2$  Sv by Richardson and Garzoli (2003) for the Benguela Drift farther downstream or the  $12 \pm 3$  Sv for its subsequent extension into the Brazil Basin (Boebel et al., 1999).

Hence, our resulting hypothesis reads as follows: Turbulent exchange, dominating the “Cape Cauldron” region reaches into the AAIW layer, and possibly below. Near the surface, high swirl velocities isolate the water in the Agulhas Rings and cyclones from the surrounding ocean while generating interleaving filaments (the stirring regime). Contrastingly, lower swirl velocities at intermediate depth open up the eddies' interior to exchange with the environment (the blender regime). This leads to a depth dependent exchange of water between the Agulhas Rings and the adjacent mesoscale cyclones, or, in other words, differential mixing rates throughout the water column. Subsequently, not only the Indian Ocean water trapped in the rings, but also the portion

<sup>7</sup>See the appendix for a discussion of ring anomaly calculations.

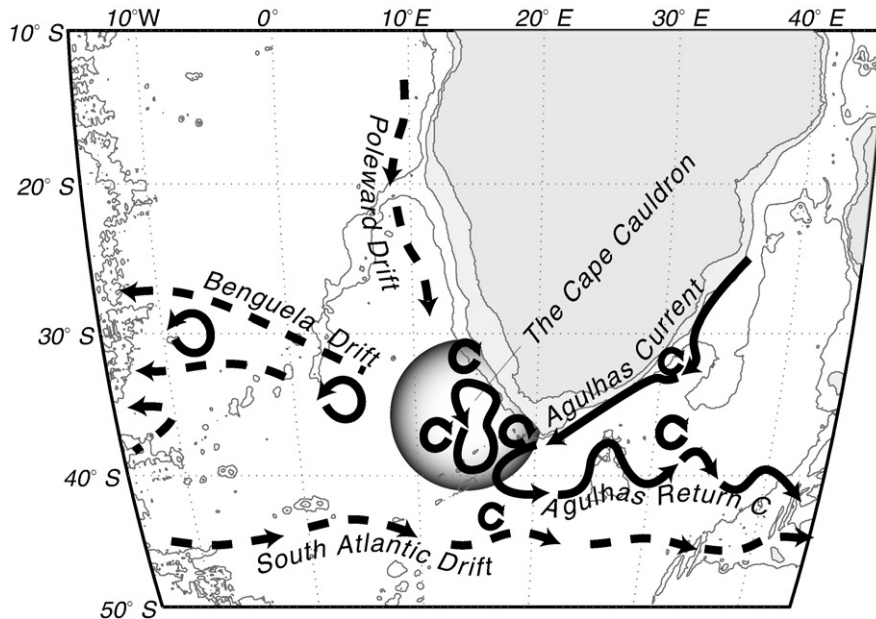


Fig. 12. Conceptual diagram for the intermediate depth inter-ocean exchange south of Africa. In deviation from the previous figures, which depicted the Cape Caudron as the box forming the geographical limits of our calculations, we chose here a circular shape for illustrative reasons.

that has been mixed into the background of the Cape Caudron while the rings reside in the latter, contributes to the inter-ocean exchange.

Fig. 12 summarizes the proposed new concepts and extends them with results from accompanying papers. Antarctic Intermediate Water, originating in the western South Atlantic is advected eastward with the South Atlantic Current (SAC). In the eastern South Atlantic this currents' strength is substantially reduced, (hence the label South Atlantic Drift). In comparison with typical SAC latitudes as observed in the western South Atlantic, in the eastern basin the South Atlantic Drift appears to be strongest farther south and has probably merged with the northern part of the Antarctic Circumpolar Current.

Eddy diffusion between the South Atlantic Drift and the Retroflection loop leads to the entrainment and cross frontal exchange of subantarctic waters and Atlantic AAIW across the Retroflection proper directly into the Cape Caudron. Similar exchanges between the South Atlantic Drift and the Agulhas Return Current (ARC) result in the injection of these latter waters AAIW

into the local Agulhas Recirculation Gyre (Boebel et al., 2003). Resulting cold core eddies (exemplified in Fig. 12 by the cyclone near 37°S, 31°E) are advected westward (Boebel et al., 2003), against the mean flow of the ARC which is contiguous to the south. Subsequent reattachment of these cyclones to meander troughs of the ARC or to the AC proper can lead to further mixing of Indian and Atlantic water, particularly at intermediate depth.

Agulhas Cyclones (Lutjeharms et al., 2003), found on the cyclonic, inshore side of the Agulhas Current, form an integral part of this system. They exhibit a cold core eddy, presumably carrying Indian Ocean Water that has been displaced considerably in the vertical (Lutjeharms et al., 2003). Drifting southwestward along the inshore side of the AC, they eventually reach the tip of the Agulhas Bank. Here they have been observed to assist in the shedding of Agulhas Rings by moving south, sometimes southeastward, between the prenatal Agulhas Ring, and the Retroflection proper. They also seem to sustain a topographically trapped, quasi-permanent cyclone

immediately adjacent to the tip of the Agulhas Bank (Lutjeharms et al., 2003). This cyclone, (shown in Fig. 12 by the cyclone near 37°S, 18°E), in turn, causes AC water to directly be drawn into the Cape Cauldron, and thus feeding Agulhas Waters into the Benguela Drift source region without the help of Agulhas Rings.

Other cyclones are locally formed in the Cape Basin along the shelf break, or emerge from the subantarctic region to the south of the Agulhas Retroflexion. All three types interact intensively with anticyclonic features (i.e. precursors of mature Agulhas Rings) in the Cape Cauldron. While doing so, the cyclones drift to the west–southwest, slowly loosing in strength and presumably ceding their waters to the Benguela Drift emerging out of the Cape Cauldron.

In this concept, the “Cape Cauldron” thus takes on an important integral role as mixer and stirrer in the Indian–Atlantic inter-ocean exchange with the interaction between cyclones and anticyclones resulting in a rapid decay of water mass anomalies introduced from the Indian Ocean into the Atlantic, particularly at intermediate depth. However, for an unambiguous proof of this concept, the kinematic features need to be directly compared with hydrographic profiles to understand what the range of properties found within cyclones and anticyclones is. The necessary extensive hydrographic program has not been part of KAPEX, but fortunately, the MODAS-2D SSH product also covers the time frame of recent hydrographic studies such as the Mixing of Agulhas Rings Experiment (MARE) and it will be interesting to see those profiles being interpreted with respect to the kinematic fields. Future projects, such as the soon to start Agulhas-South Atlantic Thermohaline Transport Experiment (ASTTEX) (Byrne, 2001, private communication) will attempt to focus on the long-term inter-ocean exchange and is expected to decipher each components’ budgets more precisely.

### Acknowledgements

Excellent support through all officers and crews of vessels involved in KAPEX is greatly appre-

ciated. These are, in alphabetical order, SA Kuswag I, SA Kuswag V, R.V. *Seward Johnson* and R.V. *Polarstern*. Further participants of KAPEX, i.e. Chris Duncombe Rae, Dave Fratantoni, Silvia Garzoli, and Phil Richardson provided indispensable support and valuable scientific discussions throughout the project. Discussions with Nelson Hogg, Anne-Marie Treguier, and Donald Olson, as well as comments from two anonymous reviewers are highly appreciated. Essential technical and scientific contributions were made by I. Ansorge, S. Becker, R. Berger, P. Bouchard, D. Carlsen, J. Fontaine, S. Anderson-Fontana, H. Hunt, J. Kemp, M. Nielsen and C. Wooding. Support from the National Science Foundation, USA, the Foundation for Research Developments, RSA, the Ministerium für Bildung, Wissenschaft, Forschung und Technologie (Germany), the Alexander-von-Humboldt Foundation (Germany) is acknowledged. MODAS work is supported by the Oceanographer of the Navy via the Space and Naval Warfare Systems Command (SPAWAR) under program element 0603207N and the Northern Gulf Littoral Initiative (NGLI) program. Bathymetric contours were extracted from the Smith and Sandwell Global Seafloor Topography (Smith and Sandwell, 1997).

### Appendix. The impact of the Cape Cauldron on the calculation of Agulhas Ring anomalies

Calculating the total inter-ocean exchange from the number of rings per year times their property anomalies depends directly on estimates of the rings’ volume and their associated anomalies. Typical choices for a rings’ volume were the amount of water found within the radius of maximum velocity (Garzoli et al., 1999) and above the 10°C isotherm (Olson and Evans, 1986) or, alternatively, 800 m (Duncombe Rae et al., 1996). These selections are subject to considerable uncertainty, both in their experimental realization and in their general appropriateness. The radius of maximum velocity is influenced, at least for the predominantly used geostrophic or cyclostrophic velocity calculations, by the choice of a reference depth of known velocity, which is mostly selected

by educated guessing. Choosing the 10°C isotherm or 800 m as the lower integration limit is disputable as such, and might not have been uninfluenced by the fact that these are the deepest surfaces captured by XBT measurements, which were frequently used to provide the necessary spatial resolution. Schmid et al.'s (2003) exemplifying analysis of a ring at a juvenile and aged stage (their Table 1) suggests a strong dependency of its estimated anomalies on the vertical integration limit, particularly during the juvenile stage. The selection of the integration limits implicitly defines the rings' trapping depth, i.e. the depth to which rings would advect Indian Ocean water with them. However, such limits may not be constant, but are likely to depend on each ring's intrinsic kinematic properties as well as those of the surrounding ocean.

The issue of trapping depth is an important one. Let us hypothesize a trapping depth that shoals from 1500 to 700 m between the initial separation point A of the ring and another point B, say in the central Cape Basin. One could then argue that the ring carries Indian Ocean water at intermediate depth into the Cape Basin, but loses it to its surroundings while within the Basin. When the ring has reached point B, it no longer bears pure Indian Ocean intermediate water. Nevertheless, by then such water has been mixed to some degree with the water intrinsic to the Cape Basin and will eventually feed into the Atlantic with the background flow, i.e. the Benguela Drift.

The initial part of such a scenario has been deemed unlikely in the Agulhas Ring census by Duncombe Rae et al. (1996) while arguing in favor of a maximum integration/trapping depth of 800 m (page 11,955): "However, anomaly sections indicate that the differences between eddy and surroundings along density surfaces are negligible below 800 m.... These eddies could not be expected to lose their burden of Agulhas water below the trapping depth in the one or two eddy diameters they had traveled since shedding... ." Or could they? While Gordon et al. (1987) did indeed find Indian Ocean intermediate water in eddies close to the retroflection, Duncombe Rae et al. (1996) argue that the trapping depth initially is at only 800 m, due to a high translation speed of the ring,

implicitly excluding the import of Indian Ocean intermediate water into the Atlantic.

However, while still connected to the Agulhas Current, the prenatal ring is continuously being provided with Indian Ocean Antarctic Intermediate Water. A shoaling of the trapping depth is expected only after the ring's detachment and in response to its first rapid displacement. As shown by Schmid et al. (2003), rings' phase velocities are variable during this early stage and hence changes in trapping depth are likely. Farther west the reverse process might occur. There an increase of trapping depth is expected (Duncombe Rae et al., 1996) when the ring moves into the northwestern part of the Cape Basin and its phase propagation slows down relative to the internal particle speed. This might be responsible for the re-trapping of intermediate water from the Cape Basin and its export into the western South Atlantic.

The resulting modification of background properties strongly influences inter-ocean exchange estimates based on the rings' heat and salt anomalies. When, in calculating the anomalies, selecting a reference station just outside a given ring, those salt and heat contents that have already been mixed into the background, i.e. that are present at the reference station, are implicitly subtracted. Thus the rings' anomalies are underestimated with regard to what was initially injected into the Atlantic during the shedding event. When extrapolating these rings' anomalies to an annual flux, the overall influence of the Indian Ocean is underestimated.

## References

- Boebel, O., Barron, C.N., 2003. A comparison of in-situ float velocities with altimeter derived geostrophic velocities. *Deep-Sea Research II*, this issue (PII:S0967-0645(02)00381-8).
- Boebel, O., Duncombe Rae, C., Garzoli, S., Lutjeharms, J., Richardson, P., Rossby, T., Schmid, C., Zenk, W., 1998. Float experiment studies interocean exchanges at the tip of Africa. *EOS* 79 (1), 6–8.
- Boebel, O., Davis, R.E., Ollitrault, M., Peterson, R.G., Richardson, P.L., Schmid, C., Zenk, W., 1999. The intermediate depth circulation of the western South Atlantic. *Geographical Research Letters* 26, 3329–3332.

- Boebel, O., Anderson-Fontana, S., Schmid, C., Ansoerge, I., Lazarevich, P., Lutjeharms, J., Prater, M., Rossby, T., Zenk, W., 2000. KAPEX RAFOS Float Data Report 1997–1999; Part A: The Agulhas- and South Atlantic Current Components, pp. 194, Institut für Meereskunde n der Christian-Albrechts-Universität-Kiel, Berichte aus dem Institut für Meereskunde 318, Kiel.
- Boebel, O., Rossby, T., Lutjeharms, J., Zenk, W., Barron, C., 2003. Path and variability of the Agulhas Return Current, *Deep-Sea Research II*, this issue (PII:S0967-0645(02)00377-6).
- Bower, A.S., 1989. Potential vorticity balances and horizontal divergence along particle trajectories in Gulf Stream meanders east of Cape Hatteras. *Journal of Physical Oceanography* 19, 1669–1681.
- Bower, A.S., Rossby, T.H., 1989. Evidence of cross-frontal exchange processes in the Gulf Stream based on isopycnal RAFOS float data. *Journal of Physical Oceanography* 19, 1177–1190.
- Byrne, D.A., Gordon, A.L., Haxby, W.F., 1994. Agulhas Eddies, a synoptic view using Geosat ERM data. *Journal of Physical Oceanography* 25, 902–917.
- Clement, A.C., Gordon, A.L., 1995. The absolute velocity field of Agulhas eddies and the Benguela Current. *Journal of Geophysical Research* 100, 22591–22601.
- de Ruijter, W.P.M., Biastoch, A., Drijfhout, S.S., Lutjeharms, J.R.E., Matano, R.P., Pichevin, T., van Leewen, P.J., Weijer, W., 1999. Indian-Atlantic interocean exchange: dynamics, estimation and impact. *Journal of Geophysical Research* 104, 20885–20910.
- Döös, K., 1995. Interocean exchange of water masses. *Journal of Geophysical Research* 100, 13499–13514.
- Duncombe Rae, C.M., Shillington, F.A., Agenbag, J.J., Taunton-Clark, J., Gründlingh, M.L., 1992. An Agulhas ring in the South Atlantic Ocean and its interaction with the Benguela upwelling frontal system. *Deep-Sea Research* 39A, 2009–2027.
- Duncombe Rae, C.M., Garzoli, S.L., Gordon, A.L., 1996. The eddy field of the southeast Atlantic Ocean: a statistical census from the Benguela sources and transports project. *Journal of Geophysical Research* 101, 11949–11964.
- Flierl, G.R., 1981. Particle motions in large-amplitude wave fields. *Geophysical Astrophysical Fluid Dynamics* 18, 39–74.
- Fox, D.N., Teague, W.J., Barron, C.N., Carnes, M.R., Lee, C.M., 2003. The Modular Ocean Data Assimilation System (MODAS). *Journal of Atmospheric and Oceanic Technology* 19, 240–252.
- Fu, L.-L., Chelton, D.B., 2001. Large-scale ocean circulation. In: Fu, L.-L., Cazenave, A. (Eds.), *Satellite Altimetry and Earth Sciences*. Academic Press, San Diego, pp. 133–169.
- Garzoli, S.L., Gordon, A.L., 1996. Origins and variability of the Benguela Current. *Journal of Geophysical Research* 101, 897–906.
- Garzoli, S.L., Richardson, P.L., Duncombe Rae, C.M., Fratantoni, D.M., Goñi, G., Roubicek, A.J., 1999. Three Agulhas rings observed during the Benguela Current experiment. *Journal of Geophysical Research* 104, 20971–20985.
- Goñi, G., Garzoli, S.L., Roubicek, A.J., Olson, D., Brown, O., 1997. Agulhas ring dynamics from TOPEX/Poseidon satellite altimeter data. *Journal of Marine Research* 55, 861–883.
- Gordon, A.L., 1986. Interocean exchange of thermocline water. *Journal of Geophysical Research* 91, 5037–5046.
- Gordon, A.L., Lutjeharms, J.R.E., Gründlingh, M.L., 1987. Stratification and circulation at the Agulhas Retroflection. *Deep-Sea Research* 34, 565–599.
- Gordon, A.L., Weiss, R.F., Smethie, W.M., Warner, M.J., 1992. Thermocline and intermediate water communication between the South Atlantic and Indian Oceans. *Journal of Geophysical Research* 97, 7223–7240.
- Gründlingh, M.L., 1995. Tracking eddies in the southeast Atlantic and southwest Indian oceans with TOPEX/Poseidon. *Journal of Geophysical Research* 100, 24977–24986.
- Gründlingh, M.L., 1999. Surface currents derived from satellite-tracked buoys off Namibia. *Deep-Sea Research II* 46, 453–473.
- Hogg, N.G., Stommel, H.M., 1985. The heton, an elementary interaction between discrete baroclinic geostrophic vortices, and its implications concerning heat-flow. *Proceedings of the Royal Society of London, A* 397, 1–20.
- Jacobs, G.A., Barron, C.N., Rhodes, R.C., 2001. Mesoscale characteristics. *Journal of Geophysical Research* 106, 19581–19596.
- Lutjeharms, J.R.E., 1981. Features of the southern Agulhas Current circulation from satellite remote sensing. *South African Journal of Science* 77, 231–236.
- Lutjeharms, J.R.E., 1996. The exchange of water between the South Indian and South Atlantic Oceans. In: Wefer, G., Berger, W.H., Siedler, G., Webb, D. (Eds.), *The South Atlantic: Present and Past Circulation*. Springer, Berlin-Heidelberg, pp. 122–162.
- Lutjeharms, J.R.E., Cooper, J., 1996. Interbasin leakage through Agulhas current filaments. *Deep-Sea Research I* 43, 213–238.
- Lutjeharms, J.R.E., Gordon, A.L., 1987. Shedding of an Agulhas ring observed at sea. *Nature* 325, 138–139.
- Lutjeharms, J.R.E., Boebel, O., Rossby, H.T., 2003. Agulhas cyclones. *Deep-Sea Research II*, this issue (PII:S0967-0645(02)00378-8).
- Matano, R., Beier, E.J., 2002. A kinematic analysis of the Indian/Atlantic interocean exchange. *Deep Sea Research II*, this issue (PII:S0967-0645(02)00395-8).
- Ollitrault, M., 1994. *The Topogolf Experiment: Lagrangian Data*. IFREMER—Centre de Brest, Editions de L’Ifremer, Brest, France.
- Olson, D.B., Evans, R.H., 1986. Rings of the Agulhas Current. *Deep Sea Research* 33, 27–42.
- Penven, P., Lutjeharms, J.R.E., Marchesiello, P., Roy, C., Weeks, S.J., 2001. Generation of cyclonic eddies by the Agulhas Current in the lee of the Agulhas Bank. *Geographical Research Letters* 27, 1055–1058.

- Richardson, P.L., Garzoli, S.L., 2003. Characteristics of Intermediate Water flow in the Benguela Current as measured with RAFOS floats. *Deep Sea Research II*, this issue (PII:S0967-0645(02)00380-6).
- Richardson, P.L., Bower, A.S., Zenk, W., 2000. A census of Meddies tracked by floats. *Progress in Oceanography* 45, 209–250.
- Rosby, T., Dorson, D., Fontaine, J., 1986. The RAFOS System. *Journal of Atmospheric and Oceanic Technology* 3, 672–679.
- Schmid, C., Siedler, G., Zenk, W., 2000. Dynamics of intermediate water circulation in the subtropical South Atlantic. *Journal of Physical Oceanography* 30, 3191–3211.
- Schmid, C., Boebel, O., Zenk, W., Lutjeharms, J., Garzoli, S.L., Richardson, P.L., Barron, C.N., 2003. Early evolution of an Agulhas Ring. *Deep-Sea Research II*, this issue (PII:S0967-0645(02)00382-X).
- Schmitz, W.J., 1996. On the eddy field in the Agulhas Retroflection, with some global considerations. *Journal of Geophysical Research* 101, 16259–16271.
- Shannon, G., Nelson, G., 1996. The Benguela: large scale features and processes and system variability. In: Wefer, G., Berger, W.H., S. G., Webb, D.J. (Eds.), *The South Atlantic: Present and Past Circulation*. Springer, Berlin Heidelberg, pp. 163–210.
- Shannon, L.V., Hunter, D., 1988. Notes on Antarctic Intermediate Water around southern Africa. *South African Journal of Marine Science* 6, 107–117.
- Siedler, G., Müller, T.J., Onken, R., Arhan, M., Mercier, H., King, B.A., Saunders, P.M., 1996. The zonal WOCE sections in the South Atlantic. In: Wefer, G., Berger, W.H., Siedler, G., Webb, D.J. (Eds.), *The South Atlantic*. Springer, Berlin-Heidelberg, pp. 83–104.
- Smith, W.H.F., Sandwell, D.T., 1997. Global seafloor topography from satellite altimetry and ship depth soundings. *Science*.
- Stramma, L., England, M., 1999. On the water masses and mean circulation of the South Atlantic Ocean. *Journal of Geophysical Research* 104, 20863–20883.
- Stramma, L., Peterson, R.G., 1989. Geostrophic transport in the Benguela Current Region. *Journal of Physical Oceanography* 19, 1440–1448.
- Stramma, L., Peterson, R.G., 1990. The South Atlantic Current. *Journal of Physical Oceanography* 20, 846–859.
- Treguier, A.-M., Boebel, O., Barnier, B., Madec, G., 2003. Agulhas eddy fluxes in a 1/6° Atlantic model. *Deep-Sea Research II*, this issue (PII:S0967-0645(02)00396-X).
- van Aken, H.M., van Veldhoven, A.K., Veth, C., de Ruijter, W.P.M., van Leeuwen, P.J., Drijfhout, S.S., Whittle, C.P., Rouault, M., 2003. Observations of a young Agulhas ring, Astrid, during MARE, the Mixing of Agulhas Rings Experiment. *Deep-Sea Research II*, this issue (PII:S0967-0645(02)00383-1).
- Watts, D.R., Rossby, H.T., 1977. Measuring dynamic heights with inverted echo sounders: results from mode. *Journal of Physical Oceanography* 7, 345–358.
- You, Y., 2002. Quantitative estimate of Antarctic Intermediate Water contributions from the Drake Passage and the southwest Indian Ocean to the South Atlantic. *Journal of Geophysical Research* 107, 10.1029/2001JC000880.
- You, Y., Lutjeharms, J., Boebel, O., de Ruijter, W.P.M., 2003. Quantification of the interocean exchange of intermediate water masses around the Cape of Good Hope. *Deep-Sea Research II*, this issue (PII:S0967-0645(02)00384-3).